mathematics

MDPI

Article

Construction of Infinite Series Exact Solitary Wave Solution of the KPI Equation via an Auxiliary Equation Method

Feiyun Pei [1], Guojiang Wu [2] and Yong Guo [2,*]

[1] School of Economics and Management, Huainan Normal University, Huainan 232038, China
[2] Institute of Plasma Physics, Hefei Institutes of Physical Science, Chinese Academy of Sciences, Hefei 230031, China
* Correspondence: yguo@ipp.ac.cn

Abstract: The KPI equation is one of most well-known nonlinear evolution equations, which was first used to described two-dimensional shallow water wavs. Recently, it has found important applications in fluid mechanics, plasma ion acoustic waves, nonlinear optics, and other fields. In the process of studying these topics, it is very important to obtain the exact solutions of the KPI equation. In this paper, a general Riccati equation is treated as an auxiliary equation, which is solved to obtain many new types of solutions through several different function transformations. We solve the KPI equation using this general Riccati equation, and construct ten sets of the infinite series exact solitary wave solution of the KPI equation. The results show that this method is simple and effective for the construction of infinite series solutions of nonlinear evolution models.

Keywords: KPI equation; auxiliary equation; nonlinear evolution equation; hyperbolic function; solitary wave solutions

MSC: 35D99

Citation: Pei, F.; Wu, G.; Guo, Y. Construction of Infinite Series Exact Solitary Wave Solution of the KPI Equation via an Auxiliary Equation Method. *Mathematics* **2023**, *11*, 1560. https://doi.org/10.3390/math11061560

Academic Editor: Nikolai A. Magnitskii

Received: 3 March 2023
Revised: 16 March 2023
Accepted: 20 March 2023
Published: 22 March 2023

1. Introduction

In modern physics and engineering, many physics phenomena, including hydrodynamics, optics, plasma, condensed matter physics, elementary particle physics, material physics, ocean engineering, astrophysics, and biology [1–6], can be expressed as nonlinear evolution equations (NLEEs) varying with time and space. A lot of methods have been proposed to obtain the exact traveling wave solutions of NLEEs, such as the F-expansion method [7–11], the tanh method and its extension [12–14], the Jacobi elliptic function method [15–18], the auxiliary equation method [19–23], the homogenous balance method [24,25], the trial function method [26], the (G′/G)-expansion method and its extension [27–30], and so on.

The Kadomtsev–Petviashvili (KP) equation [31], shown in Equation (1), was proposed by Kadomtsev and Petviashvili in 1970 to study the physical model of a two-dimensional shallow water wave, which describes how the water wave mainly propagates along the X-direction while the movement is very small in the Y-direction.

$$(u_t + 6 \cdot u \cdot u_x + u_{xxx})_x + \sigma^2 \cdot u_{yy} = 0 \tag{1}$$

This NLEE has important applications in fluid mechanics [32–34], plasma ion acoustic wave [35], nonlinear optics [36,37], and other fields. The KP equation is renamed the KPI equation when $\sigma^2 = -1$, and the KPII equation when $\sigma^2 = 1$. Compared with the KPII equation, the KPI equation has many more types of solutions [38–44]. In this work, we only discuss the solutions of KPI equation, shown as Equation (2):

$$(u_t + 6 \cdot u \cdot u_x + u_{xxx})_x - u_{yy} = 0 \tag{2}$$

To study various complex and diverse evolutionary processes of the KPI equation, we introduce a method to construct infinite series solutions of the KPI equation by using of Riccati equation as an auxiliary equation. Firstly, the general Riccati equation is solved to obtain many new types of solutions through several different function transformations. Then, we use this general Riccati equation as an auxiliary equation to solve the KPI equation. Finally, the infinite series exact solitary wave solutions are obtained. In this work, a simple Riccati equation is used to construct the form of the KPI equation's solution as $f(\xi)$ in Section 2. In Section 3, three different function transformations of $f(\xi)$ are used to obtain ten sets of infinite-series hyperbolic function solutions, which are used to construct the infinite series exact solitary wave solution of the KPI equation. In Section 4, the infinite series exact solitary wave solutions are discussed in detail. Finally, a conclusion is given in Section 5.

2. The Form of KPI Equation's Solutions

We assume that Equation (2) has the following traveling wave transformation:

$$\begin{cases} u(x,y,t) = u(\xi) \\ \xi = k_x \cdot x + k_y \cdot y + c \cdot t \end{cases} \tag{3}$$

where k_x, k_y and c are the wave number in X and Y directions and wave speed, respectively. Equation (2) can be converted to an ODE, shown as Equation (4):

$$k_x^4 \cdot u'' + \left(ck_x - k_y^2\right) \cdot u + 3k_x^2 \cdot u^2 = 0 \tag{4}$$

where u' represents $du/d\xi$. $u(\xi)$ can be assumed as a finite series of defined $f(\xi)$, shown as Equation (5):

$$(\xi) = \sum_{j=0}^{n} a_j \cdot f^n(\xi) \tag{5}$$

where a_j are constants, $f(\xi)$ is the solution to be constructed later, and n can be obtained by the homogeneous balance between u'' and u^2 in Equation (4).

The highest degree of $d^p u/d\xi^p$ is taken as:

$$O(d^p u/d\xi^p) = n + p, \quad p = 1, 2, 3 \cdots \tag{6}$$

We can obtain $n = 2$, and $u(\xi)$ can be expressed as:

$$u(\xi) = a_0 + a_1 \cdot f(\xi) + a_2 \cdot f^2(\xi) \tag{7}$$

a_0, a_1 and a_2 in Equation (7) are constants to be determined later, and $f(\xi)$ is defined by simple Riccati equation, shown as:

$$f'(\xi) = f^2(\xi) + \mu \tag{8}$$

Substituting Equation (8) into Equation (4), and setting the coefficients of $f^n(\xi)$ to zero, we get the following equation:

$$\begin{cases} 6k_x^4 \cdot a_2 + 3k_x^2 \cdot a_2^2 = 0 \\ 2k_x^4 \cdot a_1 + 6k_x^2 \cdot a_1 a_2 = 0 \\ 8k_x^4 \cdot \mu a_2 + ck_x \cdot a_2 - k_y^2 \cdot a_2 + 3k_x^2 \cdot a_1^2 + 6k_x^2 \cdot a_0 a_2 = 0 \\ 2k_x^4 \cdot \mu a_1 + ck_x \cdot a_1 - k_y^2 \cdot a_1 + 6k_x^2 \cdot a_0 a_1 = 0 \\ 2k_x^4 \cdot \mu^2 a_2 + ck_x \cdot a_0 - k_y^2 \cdot a_0 + 3k_x^2 \cdot a_0^2 = 0 \end{cases} \tag{9}$$

By solving these equations, we obtain the two solutions, shown as Equation (10):

$$\begin{cases} a_0 = -\left(2k_x^2 \cdot \mu\right)/3 \\ a_1 = 0 \\ a_2 = -2k_x^2 \\ c = \left(k_y^2 - 4k_x^4 \cdot \mu\right)/k_x \\ k_x \neq 0 \\ k_y \neq 0 \end{cases} \text{ or } \begin{cases} a_0 = -2k_x^2 \cdot \mu \\ a_1 = 0 \\ a_2 = -2k_x^2 \\ c = \left(k_y^2 + 4k_x^4 \cdot \mu\right)/k_x \\ k_x \neq 0 \\ k_y \neq 0 \end{cases} \tag{10}$$

$u(\xi)$ could be expressed as $v(\xi)$ in Equation (11) and $w(\xi)$ in Equation (12):

$$\begin{cases} v(\xi) = -\left(2k_x^2 \cdot \mu\right)/3 - 2k_x^2 \cdot f^2(\xi) \\ \xi = k_x \cdot x + k_y \cdot y + \left(k_y^2 - 4k_x^4 \cdot \mu\right)/k_x \cdot t \end{cases} \tag{11}$$

$$\begin{cases} w(\xi) = -2k_x^2 \cdot \mu - 2k_x^2 \cdot f^2(\xi) \\ \xi = k_x \cdot x + k_y \cdot y + \left(k_y^2 + 4k_x^4 \cdot \mu\right)/k_x \cdot t \end{cases} \tag{12}$$

where $k_x \neq 0$ and $k_y \neq 0$. Obviously, in order to get the solution of $u(\xi)$, we need to supplement the definition of $f(\xi)$ to obtain the form of $f(\xi)$ and the value of μ.

3. The Definition of $f(\xi)$

According to Equations (11) and (12), different sets of solutions $u(\xi)$ could be determined through different definitions of $f(\xi)$. In the following, we adopt three definitions of $f(\xi)$ to obtain ten sets of infinite-series hyperbolic function solutions for the KPI equation.

3.1. The First Definition of $f(\xi)$

$f(\xi)$ is defined as Equation (13):

$$f(\xi) = k_0 + k_1 \cdot g_n'(\xi)/[g_n(\xi) + r] \tag{13}$$

where k_0, k_1, r are constants to be determined later.

While $g_n(\xi)$ is defined as Equation (14), and p_n and q_n are constants in these equations.

$$\left[g_n'(\xi)\right]^2 = p_n \cdot {g_n}^2(\xi) + q_n \tag{14}$$

When $n = 0$, $[g_0'(\xi)]^2 = p_0 \cdot {g_0}^2(\xi) + q_0$. Obviously, this equation has three solutions:

$$\begin{cases} g_{01}(\xi) = sinh(\xi) & (p_0 = 1, q_0 = 1) \\ g_{02}(\xi) = cosh(\xi) & (p_0 = 1, q_0 = -1) \\ g_{03}(\xi) = sinh(\xi) + \varepsilon \cdot cosh(\xi) & \left(p_0 = 1, q_0 = 0, \varepsilon^2 = 1\right) \end{cases} \tag{15}$$

By substituting Equation (13) into Equation (8), using Equation (14), and then setting each coefficient of ${g_n}^i(\xi)$ $(i = 0, 1, 2, \cdots)$ to zero, the following equations can be obtained.

$$\begin{cases} k_0 = 0, \\ {k_1}^2 p_n + \mu = 0, \\ k_1 p_n r = 2\mu r, \\ -k_1 q_n = {k_1}^2 q_n + \mu r^2; \end{cases} \text{ or } \begin{cases} q_n = 0, \\ {k_0}^2 + {k_1}^2 p_n \pm 2k_0 k_1 \sqrt{p_n} + \mu = 0, \\ k_1 p_n r = 2{k_0}^2 r \pm 2k_0 k_1 r \sqrt{p_n} + 2\mu r, \\ {k_0}^2 r^2 + \mu r^2 = 0. \end{cases} \tag{16}$$

Solving them, we can obtain Equation (17).

$$\begin{cases} k_0 = 0, \\ k_1 = -\frac{1}{2}, \\ \mu = -\frac{p_n}{4}, \\ r = \pm\sqrt{-\frac{q_n}{p_n}}; \end{cases} \quad \text{or} \quad \begin{cases} q_n = 0, \\ k_0 = \pm\frac{1}{2}\sqrt{p_n} \\ k_1 = -1, \\ \mu = -\frac{p_n}{4}, \\ r \neq 0. \end{cases} \tag{17}$$

The constants p_n and q_n in Equation (14) are the key to obtain the values of constants k_0, k_1 and r in Equation (13), so as to determine the $f(\xi)$. Therefore, two recursive relations of $g_n(\xi)$ are introduced below:

Case 1:

$$g_n(\xi) = {g_{n-1}}^2(\xi) + a_{n-1} \tag{18}$$

For $n = 1$:

$$\begin{cases} \left[g_1'(\xi)\right]^2 = p_1 \cdot {g_1}^2(\xi) + q_1 \\ g_1(\xi) = {g_0}^2(\xi) + a_0 \end{cases} \tag{19}$$

We obtain the following numerical relationship:

$$\begin{cases} 4p_0 = p_1, \\ 4q_0 = 2p_1 a_0, \\ p_1 {a_0}^2 + q_1 = 0 \end{cases} \tag{20}$$

Solving these equations, we get:

$$\begin{cases} p_1 = 4p_0 \\ q_1 = -{q_0}^2 / p_0 \\ a_0 = q_0 / (2 \cdot p_0) \end{cases} \tag{21}$$

$$\begin{cases} g_{11}(\xi) = sinh^2(\xi) + \frac{1}{2} & (p_0 = 4, q_0 = -1) \\ g_{12}(\xi) = cosh^2(\xi) - \frac{1}{2} & (p_0 = 4, q_0 = -1) \\ g_{13}(\xi) = [sinh(\xi) + \varepsilon \cdot cosh(\xi)]^2 & \left(p_0 = 4, q_0 = 0, \varepsilon^2 = 1\right) \end{cases} \tag{22}$$

For $n \geq 2$:

Due to $sinh^2(\xi) + \frac{1}{2} = cosh^2(\xi) - \frac{1}{2}$, the infinite series hyperbolic function solutions for $g_{n1}(\xi)$ are the same as that for $g_{n2}(\xi)$. It is easy to obtain mathematical recurrence formula satisfying Equation (14), shown in Equation (23):

$$g_n(\xi) = {g_{n-1}}^2(\xi) + \frac{q_{n-1}}{2p_{n-1}}, \ (p_n = 4p_{n-1}, q_n = -\frac{{q_{n-1}}^2}{p_{n-1}}). \tag{23}$$

We obtain two sets of infinite-series hyperbolic function. The first set is shown as Equation (24):

$$\begin{cases} f_{1n}(\xi) = -\frac{{g_{n-1}}'(\xi)}{2\left[g_{n-1}(\xi) \pm \sqrt{-q_{n-1}/p_{n-1}}\right]} & (\mu = -p_{n-1}/4, n = 1, 2, 3, \cdots) \\ g_n(\xi) = {g_{n-1}}^2(\xi) + q_{n-1}/(2 \cdot p_{n-1}) & \left(p_n = 4 \cdot p_{n-1}, q_n = -{q_{n-1}}^2 / p_{n-1}\right) \end{cases} \tag{24}$$

The corresponding equations of $n = 0$ are $g_0(\xi) = sinh(\xi)$ when $p_0 = 1$ and $q_0 = 1$ and $g_0(\xi) = cosh(\xi)$ when $p_0 = 1$ and $q_0 = -1$.

The second set is shown as Equation (25):

$$f_{2n}(\xi) = \pm\frac{1}{2}\nu n - \frac{\varepsilon \nu n [sinh(\xi) + \varepsilon \cdot cosh(\xi)]^{\nu n}}{[sinh(\xi) + \varepsilon \cdot cosh(\xi)]^{\nu n} + r} \quad (n = 1, 2, 3, \cdots) \tag{25}$$

where $\mu = -\left(\nu^2 \cdot n^2\right)/4$, $r \neq 0$, $\nu \neq 0$, $\varepsilon^2 = 1$.

Case 2:

$$g_n(\xi) = \sqrt{g_{n-1}(\xi) + a_{n-1}} \tag{26}$$

For $n = 1$:

$$\begin{cases} \left[g_1'(\xi)\right]^2 = p_1 \cdot {g_1}^2(\xi) + q_1 \\ g_1(\xi) = \sqrt{g_0(\xi) + a_0} \end{cases} \tag{27}$$

We obtain the following numerical relationship:

$$\begin{cases} p_0/4 = p_1 \\ 2p_1a_0 + q_1 = 0 \\ q_0/4 = p_1{a_0}^2 + q_1a_0 \end{cases} \tag{28}$$

Solving these equations, we get:

$$\begin{cases} p_1 = p_0/4 \\ q_1 = \pm 2\sqrt{-p_0q_0} \\ a_0 = \mp\sqrt{-q_0/p_0} \end{cases} \tag{29}$$

$$\begin{cases} g_{14}(\xi) = \sqrt{sinh(\xi) + \varepsilon} & \left(p_1 = 1/4, q_1 = -\varepsilon/2, \varepsilon^2 = -1\right) \\ g_{15}(\xi) = \sqrt{cosh(\xi) + \varepsilon} & \left(p_1 = 1/4, q_1 = -\varepsilon/2, \varepsilon^2 = 1\right) \\ g_{16}(\xi) = \sqrt{sinh(\xi) \pm cosh(\xi)} & \left(p_1 = \frac{1}{4}, q_1 = 0\right) \end{cases} \tag{30}$$

For $n \geq 2$:

It is easy to obtain mathematical recurrence formula satisfying Equation (14), shown as Equation (31):

$$g_n(\xi) = \sqrt{g_{n-1}(\xi) \pm \sqrt{-q_{n-1}/p_{n-1}}}, \quad \left(p_n = p_{n-1}/4, q_n = \mp\sqrt{-p_{n-1} \cdot q_{n-1}}/2\right) \tag{31}$$

Besides one set of infinite series hyperbolic function solutions being the same to Equation (25), a new set of infinite series hyperbolic function solutions is provided in this case.

$$\begin{cases} f_{3n}(\xi) = -\frac{{g_{n-1}}'(\xi)}{2\left[g_{n-1}(\xi) \pm \sqrt{-q_{n-1}/p_{n-1}}\right]} & (\mu = -p_{n-1}/4, n = 1, 2, 3, \cdots) \\ g_n(\xi) = \sqrt{g_{n-1}(\xi) \pm \sqrt{-q_{n-1}/p_{n-1}}} & (p_n = p_{n-1}/4, q_n = \mp 2\sqrt{-p_{n-1} \cdot q_{n-1}}) \end{cases} \tag{32}$$

The corresponding equations of $n = 0$ are $g_0(\xi) = sinh(\xi)$ when $p_0 = 1$ and $q_0 = 1$ and $g_0(\xi) = cosh(\xi)$ when $p_0 = 1$ and $q_0 = -1$.

3.2. The Second Definition of $f(\xi)$

$f(\xi)$ is defined as Equation (20):

$$f(\xi) = k_0 + k_1 \cdot g_n(\xi) \cdot g_n'(\xi) / \left[{g_n}^2(\xi) + r\right] \tag{33}$$

where k_0, k_1, r are constants to be determined later. Similar to Section 3.1, substituting Equation (33) into Equation (8) and use Equation (14), we get Equation (34), which provides two sets solutions shown as Equation (35):

$$\begin{cases} k_0 = 0 \\ {k_1}^2 p_n + \mu = 0 \\ -k_1q_n + 2k_1p_nr = {k_1}^2q_n + 2\mu r \\ k_1q_nr = \mu r^2 \end{cases} \text{ or } \begin{cases} q_n = 0 \\ {k_0}^2 + {k_1}^2 p_n \pm 2k_0k_1\sqrt{p_n} + \mu = 0 \\ 2k_1p_nr = 2{k_0}^2 r \pm 2k_0k_1r\sqrt{p_n} + 2\mu r \\ {k_0}^2r^2 + \mu r^2 = 0 \end{cases} \tag{34}$$

$$\begin{cases} k_0 = 0 \\ k_1 = -1 \\ \mu = -p_n \\ r = q_n/p_n \end{cases} \quad \text{or} \quad \begin{cases} q_n = 0 \\ k_0 = \pm\sqrt{p_n} \\ k_1 = -2 \\ \mu = -p_n \\ r \neq 0 \end{cases} \tag{35}$$

Corresponding to the first definition of $g_n(\xi)$ in Section 3.1, shown as Equation (18), two new sets of infinite-series hyperbolic function solutions are obtained, shown as Equations (36) and (37):

$$\begin{cases} f_{4n}(\xi) = -\frac{g_{n-1}(\xi)g_{n-1}{}'(\xi)}{g_{n-1}{}^2(\xi)+q_{n-1}/p_{n-1}} & (\mu = -p_{n-1}, n = 1,2,3,\cdots) \\ g_n(\xi) = g_{n-1}{}^2(\xi) + q_{n-1}/(2\cdot p_{n-1}) & (p_n = 4\cdot p_{n-1}, q_n = -q_{n-1}{}^2/p_{n-1}) \end{cases} \tag{36}$$

The corresponding equations of $n = 0$ are $g_0(\xi) = sinh(\xi)$ when $p_0 = 1$ and $q_0 = 1$ and $g_0(\xi) = cosh(\xi)$ when $p_0 = 1$ and $q_0 = -1$.

$$f_{5n}(\xi) = \pm\nu n - \frac{2\varepsilon\nu n[\sinh(\xi)+\varepsilon\cdot cosh(\xi)]^{2\nu n}}{[\sinh(\xi)+\varepsilon\cdot cosh(\xi)]^{2\nu n}+r} \quad (n = 1,2,3,\cdots) \tag{37}$$

where $\mu = -\nu^2 n^2$, $r \neq 0$, $\nu \neq 0$, $\varepsilon^2 = 1$.

Corresponding to the second definition of $g_n(\xi)$ in Section 3.1, shown as Equation (26), the infinite series hyperbolic function solutions are same to the $f_{3n}(\xi)$ and $f_{5n}(\xi)$, we do not get new form of solution.

3.3. The Third Definition of $f(\xi)$

Obviously, the function $a_1/f(\xi)$ also satisfies Equation (8) when $a_1 = -\mu$. We can easily obtain five new sets of infinite-series hyperbolic function solutions, which are shown below:

$$\begin{cases} f_{6n}(\xi) = -\frac{p_{n-1}[g_{n-1}(\xi)+r]}{2g_{n-1}{}'(\xi)} & (\mu = -p_{n-1}/4, r = \pm\sqrt{-q_{n-1}/p_{n-1}}) \\ g_n(\xi) = g_{n-1}{}^2(\xi) + q_{n-1}/(2\cdot p_{n-1}) & (p_n = 4\cdot p_{n-1}, q_n = -q_{n-1}{}^2/p_{n-1}) \end{cases} \tag{38}$$

where $n = 1,2,3,\cdots$. The corresponding equations of $n = 0$ are $g_0(\xi) = sinh(\xi)$ when $p_0 = 1$ and $q_0 = 1$ and $g_0(\xi) = cosh(\xi)$ when $p_0 = 1$ and $q_0 = -1$.

$$f_{7n}(\xi) = \frac{\nu n[sinh(\xi)+\varepsilon\cdot cosh(\xi)]^{\nu n}+\nu nr}{(\pm 2-4\varepsilon)[sinh(\xi)+\varepsilon\cdot cosh(\xi)]^{\nu n}\pm 2r} \quad (n = 1,2,3,\cdots) \tag{39}$$

where $\mu = -\left(\nu^2\cdot n^2\right)/4$, $r \neq 0$, $\nu \neq 0$, $\varepsilon^2 = 1$.

$$\begin{cases} f_{8n}(\xi) = -\frac{p_{n-1}[g_{n-1}(\xi)+r]}{2g_{n-1}{}'(\xi)} & (\mu = -p_{n-1}/4, r = \pm\sqrt{-q_{n-1}/p_{n-1}}) \\ g_n(\xi) = \sqrt{g_{n-1}(\xi) \pm \sqrt{-q_{n-1}/p_{n-1}}} & (p_n = p_{n-1}/4, q_n = \mp 2\sqrt{-p_{n-1}\cdot q_{n-1}}) \end{cases} \tag{40}$$

where $n = 1,2,3,\cdots$. The corresponding equations of $n = 0$ are $g_0(\xi) = sinh(\xi)$ when $p_0 = 1$ and $q_0 = 1$ and $g_0(\xi) = cosh(\xi)$ when $p_0 = 1$ and $q_0 = -1$.

$$\begin{cases} f_{9n}(\xi) = -\frac{p_{n-1}[g_{n-1}{}^2(\xi)+r]}{g_{n-1}(\xi)g_{n-1}{}'(\xi)} & (\mu = -p_{n-1}, r = q_{n-1}/p_{n-1}) \\ g_n(\xi) = g_{n-1}{}^2(\xi) + q_{n-1}/(2\cdot p_{n-1}) & (p_n = 4\cdot p_{n-1}, q_n = -q_{n-1}{}^2/p_{n-1}) \end{cases} \tag{41}$$

where $n = 1,2,3,\cdots$. The corresponding equations of $n = 0$ are $g_0(\xi) = sinh(\xi)$ when $p_0 = 1$ and $q_0 = 1$ and $g_0(\xi) = cosh(\xi)$ when $p_0 = 1$ and $q_0 = -1$.

$$f_{Xn}(\xi) = \frac{\nu n[sinh(\xi)+\varepsilon\cdot cosh(\xi)]^{2\nu n}+\nu nr}{(\pm 1-2\varepsilon)[sinh(\xi)+\varepsilon\cdot cosh(\xi)]^{2\nu n}\pm r} \quad (n = 1,2,3,\cdots) \tag{42}$$

where $\mu = -\nu^2 n^2$, $r \neq 0$, $\nu \neq 0$, $\varepsilon^2 = 1$.

Through the definition of three different functional forms of $f(\xi)$, we obtain ten sets of infinite-series hyperbolic function solutions satisfying the Riccati equation (Equation (8)), which provide the base for the solution for the KPI equation shown as Equation (7).

4. The Discussion of $u(\xi)$

Due to the space limitation of the article, we only discuss $n \leq 4$ of the ten sets of infinite-series hyperbolic function solutions $v(\xi)$ and $w(\xi)$ shown as Equations (11) and (12). Because the wave described by The KPI equation mainly propagates along the X-direction, we only consider $v(\xi)$ and $w(\xi)$ vs. (x,t) by assuming $y = 0$.

4.1. The First Set of Solutions

According to the Equation (15), $g_{01}(\xi) = sinh(\xi)$ when $p_0 = 1$ and $q_0 = 1$ and $g_{02}(\xi) = cosh(\xi)$ when $p_0 = 1$ and $q_0 = -1$. When $n \geq 1$, $g_{n1}(\xi)$ are the same as $g_{n2}(\xi)$. So, we only discuss the case of $g_{02}(\xi) = cosh(\xi)$ here, and discard the imaginary number solutions. When $n = 1$, we get Equations (43) and (44).

$$\begin{cases} f_{11}(\xi) = -\frac{sinh(\xi)}{2[cosh(\xi)+r]} & (\mu = -1/4, r = \pm 1) \\ g_1(\xi) = cosh^2(\xi) - 1/2 & (p_1 = 4, q_1 = -1) \end{cases} \tag{43}$$

$$\begin{cases} v_{11}(\xi) = \frac{k_x^2}{6} - \frac{k_x^2 \cdot sinh^2(\xi)}{2 \cdot [cosh(\xi)+r]^2} \\ \xi = k_x \cdot x + k_y \cdot y + \left(k_y^2 + k_x^4\right)/k_x \cdot t \end{cases} \text{ and } \begin{cases} w_{11}(\xi) = \frac{k_x^2}{2} - \frac{k_x^2 \cdot sinh^2(\xi)}{2 \cdot [cosh(\xi)+r]^2} \\ \xi = k_x \cdot x + k_y \cdot y + \left(k_y^2 - k_x^4\right)/k_x \cdot t \end{cases} \tag{44}$$

For the convivence of description, we assume $k_x = 1$, $k_y = 1$ and $r = 1$. Figure 1 shows bright solitary wave evolution of $v_{11}(\xi)$ (left figure) and $w_{11}(\xi)$ (right figure) vs. (x,t). The structure of these two solitary waves is roughly the same, except for the amplitude and the position of the wave crest. The difference between $v_{11}(\xi)$ and $w_{11}(\xi)$ is caused by the constant terms and the coefficient of t, which will not affect the general structure of solitary waves.

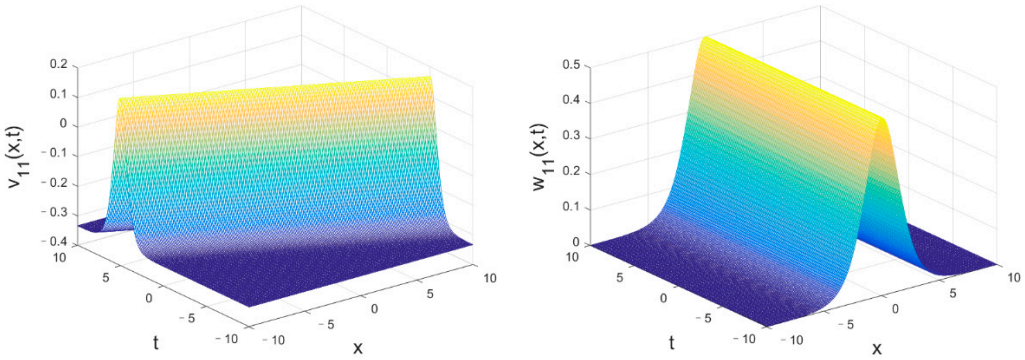

Figure 1. Bright solitary wave evolution of $v_{11}(\xi)$ (**left figure**) and $w_{11}(\xi)$ (**right figure**) vs. (x,t) when $k_x = 1$, $k_y = 1$, $r = 1$ and $y = 0$.

When $n = 2$, we get Equations (45) and (46).

$$\begin{cases} f_{12}(\xi) = -\frac{sinh(\xi) \cdot cosh(\xi)}{cosh^2(\xi) - 1/2 + r} & (\mu = -1, r = \pm 1/2) \\ g_2(\xi) = cosh^4(\xi) - cosh^2(\xi) + 1/8 & (p_2 = 16, q_2 = -1/4) \end{cases} \tag{45}$$

$$\begin{cases} v_{12}(\xi) = \frac{2k_x^2}{3} - \frac{2k_x^2 \cdot sinh^2(\xi) \cdot cosh^2(\xi)}{\left[cosh^2(\xi) - 1/2 + r\right]^2} \\ \xi = k_x \cdot x + k_y \cdot y + \left(k_y^2 + 4k_x^4\right)/k_x \cdot t \end{cases} \text{ and } \begin{cases} w_{12}(\xi) = 2k_x^2 - \frac{2k_x^2 \cdot sinh^2(\xi) \cdot cosh^2(\xi)}{\left[cosh^2(\xi) - 1/2 + r\right]^2} \\ \xi = k_x \cdot x + k_y \cdot y + \left(k_y^2 - 4k_x^4\right)/k_x \cdot t \end{cases} \tag{46}$$

Bright solitary wave evolutions of $v_{12}(\xi)$ (left figure) and $w_{12}(\xi)$ (right figure) are shown as Figure 2.

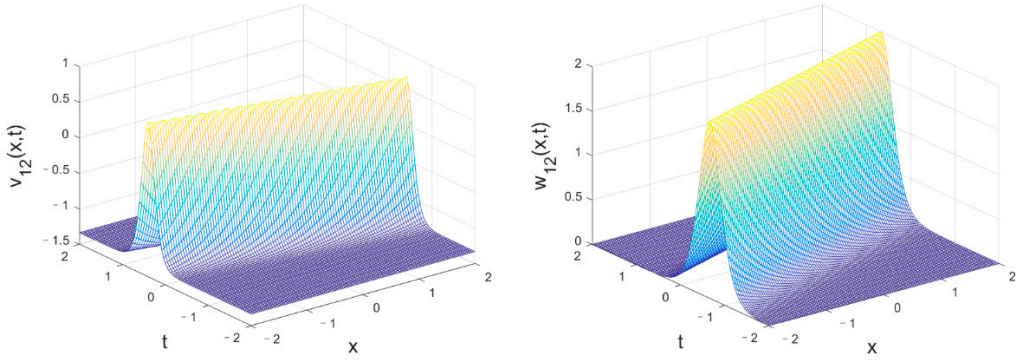

Figure 2. Bright solitary wave evolution of $v_{12}(\xi)$ (**left figure**) and $w_{12}(\xi)$ (**right figure**) vs. (x,t) when $k_x = 1, k_y = 1, r = 1/2$ and $y = 0$.

When $n = 3$, we get Equations (47)–(49). Bright solitary wave evolutions of $v_{13}(\xi)$ (left figure) and $w_{13}(\xi)$ (right figure) are shown as Figure 3:

$$\begin{cases} f_{13}(\xi) = \frac{2\cdot sinh(\xi)\cdot cosh^3(\xi) - sinh(\xi)\cdot cosh(\xi)}{cosh^4(\xi) - cosh^2(\xi) + 1/8 + r} \\ g_3(\xi) = cosh^8(\xi) - 2\cdot cosh^6(\xi) + \frac{5}{4}\cdot cosh^4(\xi) - \frac{1}{4}\cdot cosh^2(\xi) + \frac{1}{128} \\ \left(\mu = -4, r = \pm\frac{1}{8}, p_3 = 64, q_2 = -\frac{1}{256}\right) \end{cases} \tag{47}$$

$$\begin{cases} v_{13}(\xi) = \frac{8k_x^2}{3} - 2k_x^2\cdot\frac{4cosh^8(\xi) - 8cosh^6(\xi) + 5cosh^4(\xi) - cosh^2(\xi)}{\left[cosh^4(\xi) - cosh^2(\xi) + \frac{1}{8} + r\right]^2} \\ \xi = k_x\cdot x + k_y\cdot y + \left(k_y^2 + 16k_x^4\right)/k_x\cdot t \end{cases} \tag{48}$$

$$\begin{cases} w_{13}(\xi) = 8k_x^2 - 2k_x^2\cdot\frac{4cosh^8(\xi) - 8cosh^6(\xi) + 5cosh^4(\xi) - cosh^2(\xi)}{\left[cosh^4(\xi) - cosh^2(\xi) + \frac{1}{8} + r\right]^2} \\ \xi = k_x\cdot x + k_y\cdot y + \left(k_y^2 - 16k_x^4\right)/k_x\cdot t \end{cases} \tag{49}$$

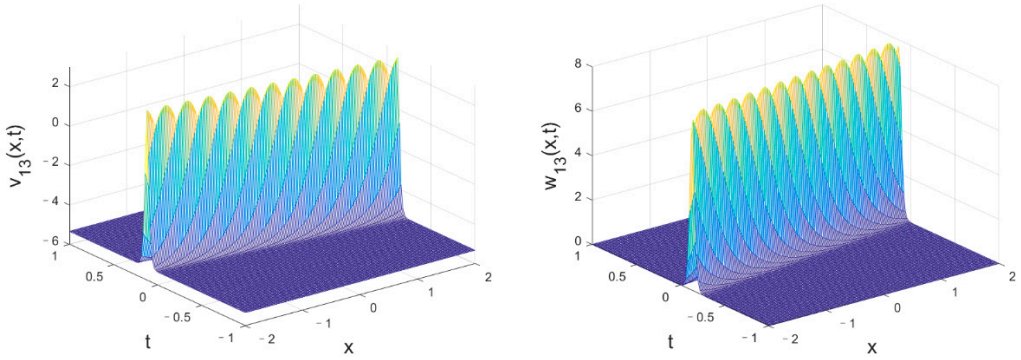

Figure 3. Bright solitary wave evolution of $v_{13}(\xi)$ (**left figure**) and $w_{13}(\xi)$ (**right figure**) vs. (x,t) when $k_x = 1, k_y = 1, r = 1/8$ and $y = 0$.

When $n = 4$, we get Equations (50)–(52). Solitary wave evolutions of $v_{14}(\xi)$ (left figure) and $w_{14}(\xi)$ (right figure) are shown in Figure 4.

$$\begin{cases} f_{14}(\xi) = \frac{8\cdot sinh(\xi)\cdot cosh^7(\xi) - 12\cdot sinh(\xi)\cdot cosh^5(\xi) + 5\cdot sinh(\xi)\cdot cosh^3(\xi) - sinh(\xi)\cdot cosh(\xi)/2}{2\cdot\left[cosh^8(\xi) - 2\cdot cosh^6(\xi) + \frac{5}{4}\cdot cosh^4(\xi) - \frac{1}{4}\cdot cosh^2(\xi) + \frac{1}{128} + r\right]} \\ g_4(\xi) = \left[cosh^8(\xi) - 2\cdot cosh^6(\xi) + \frac{5}{4}\cdot cosh^4(\xi) - \frac{1}{4}\cdot cosh^2(\xi) + \frac{1}{128}\right]^2 - \frac{1}{32768} \\ \left(\mu = -16, r = \pm\frac{1}{128}, p_4 = 256, q_4 = -\frac{1}{4194304}\right) \end{cases} \tag{50}$$

$$\begin{cases} v_{14}(\xi) = \frac{32\cdot k_x^2}{3} - k_x^2 \cdot \frac{32\left[cosh^8(\xi) - 2cosh^6(\xi) + \frac{5}{4}cosh^4(\xi) - \frac{1}{4}cosh^2(\xi) - \frac{7}{64}\right]^2 - \frac{1}{512}}{\left[cosh^8(\xi) - 2cosh^6(\xi) + \frac{5}{4}cosh^4(\xi) - \frac{1}{4}cosh^2(\xi) - \frac{7}{64} + r\right]^2} \\ \xi = k_x\cdot x + k_y\cdot y + \left(k_y^2 + 64k_x^4\right)/k_x\cdot t \end{cases} \tag{51}$$

$$\begin{cases} w_{14}(\xi) = 32\cdot k_x^2 - k_x^2 \cdot \frac{32\left[cosh^8(\xi) - 2cosh^6(\xi) + \frac{5}{4}cosh^4(\xi) - \frac{1}{4}cosh^2(\xi) - \frac{7}{64}\right]^2 - \frac{1}{512}}{\left[cosh^8(\xi) - 2cosh^6(\xi) + \frac{5}{4}cosh^4(\xi) - \frac{1}{4}cosh^2(\xi) - \frac{7}{64} + r\right]^2} \\ \xi = k_x\cdot x + k_y\cdot y + \left(k_y^2 - 64k_x^4\right)/k_x\cdot t \end{cases} \tag{52}$$

With the increase of n in $v_{1n}(\xi)$ and $w_{1n}(\xi)$, the amplitude of $v_{1n}(\xi)$ and $w_{1n}(\xi)$ increases, and the bandwidth in space–time decreases.

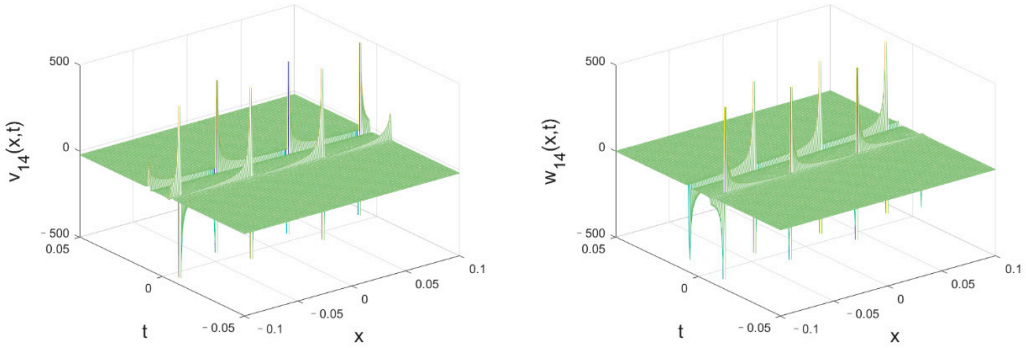

Figure 4. Solitary wave evolution of $v_{14}(\xi)$ (**left figure**) and $w_{14}(\xi)$ (**right figure**) vs. (x,t) when $k_x = 1, k_y = 1, r = 1/128$ and $y = 0$.

4.2. The Second Set of Solution

According to $f_{2n}(\xi)$ given by Equation (25), the second set of solution $u_{2n}(\xi)$ is given by Equation (53).

$$\begin{cases} u_{2n}(\xi) = \left(-\frac{1}{6} \pm \frac{1}{6}\right)\nu^2 n^2 k_x^2 + \frac{2\lambda k_x^2 \nu^2 n^2 [sinh(\xi) + \varepsilon\cdot cosh(\xi)]^{\nu n}}{[sinh(\xi) + \varepsilon\cdot cosh(\xi)]^{\nu n} + r} - 2\left\{\frac{k_x \nu n [sinh(\xi) + \varepsilon\cdot cosh(\xi)]^{\nu n}}{[sinh(\xi) + \varepsilon\cdot cosh(\xi)]^{\nu n} + r}\right\}^2 \\ \left(\ \xi = k_x x + k_y y + ct, c = \left(k_y^2 \mp \nu^2 n^2 k_x^4\right)/k_x, \mu = -\frac{\nu^2\cdot n^2}{4}, \lambda^2 = 1, \varepsilon^2 = 1\ \right) \end{cases} \tag{53}$$

Here, we only consider the case of $\lambda = 1, \nu = 1, \varepsilon = 1$ and $r = 1$. The expressions of $v(\xi)$ and $w(\xi)$ are shown as Equations (54) and (55):

$$\begin{cases} v_{2n}(\xi) = -\frac{1}{3}n^2 k_x^2 + \frac{2k_x^2 n^2 [sinh(\xi) + cosh(\xi)]^n}{[sinh(\xi) + cosh(\xi)]^n + 1} - 2\left\{\frac{k_x n [sinh(\xi) + cosh(\xi)]^n}{[sinh(\xi) + cosh(\xi)]^n + 1}\right\}^2 \\ \xi = k_x\cdot x + k_y\cdot y + \left(k_y^2 + n^2 k_x^4\right)/k_x\cdot t \end{cases} \tag{54}$$

$$\begin{cases} w_{2n}(\xi) = \frac{2k_x^2 n^2 [sinh(\xi) + cosh(\xi)]^n}{[sinh(\xi) + cosh(\xi)]^n + 1} - 2\left\{\frac{k_x n [sinh(\xi) + cosh(\xi)]^n}{[sinh(\xi) + cosh(\xi)]^n + 1}\right\}^2 \\ \xi = k_x\cdot x + k_y\cdot y + \left(k_y^2 - n^2 k_x^4\right)/k_x\cdot t \end{cases} \tag{55}$$

Figures 5–8 show the structure of bright solitary wave of Equations (54) and (55) when $n = 1$ to 4. Under these conditions, with the increase of n, the amplitude of the bright solitary wave increases and the bandwidth in space–time decreases. The solitary wave structure is relatively stable under low-n conditions. Under high-n conditions, $v_{2n}(\xi)$ and $w_{2n}(\xi)$ increase sharply in a small space–time range and becomes unstable.

4.3. The Third Set of Solutions

Here, we only consider the examples corresponding to $g_0(\xi) = cosh(\xi)$. According to the recurrence relation of Equation (32), we obtain the expressions of $f_{3n}(\xi)$ and $g_n(\xi)$ corresponding to different n. These expressions are brought into Equations (11) and (12) to find the two solutions $v(\xi)$ and $w(\xi)$. The cases of $n \leq 4$ are shown below.

When $n = 1$, Equation (56) is the same as Equation (44), in which $r = \pm 1$. The solutions are shown as Figure 1, which will not be repeated here.

$$\begin{cases} v_{31}(\xi) = \frac{k_x^2}{6} - \frac{k_x^2 \cdot sinh^2(\xi)}{2 \cdot [cosh(\xi)+r]^2} \\ \xi = k_x \cdot x + k_y \cdot y + \left(k_y^2 + k_x^4\right)/k_x \cdot t \end{cases} \text{and} \begin{cases} w_{31}(\xi) = \frac{k_x^2}{2} - \frac{k_x^2 \cdot sinh^2(\xi)}{2 \cdot [cosh(\xi)+r]^2} \\ \xi = k_x \cdot x + k_y \cdot y + \left(k_y^2 - k_x^4\right)/k_x \cdot t \end{cases} \quad (56)$$

When $n = 2$, the solutions are shown as Equation (57), in which $r = \pm 2\sqrt{2}$. The corresponding solitary wave evolution is shown as Figure 9 with $k_x = 1$, $k_y = 1$ and $y = 0$.

$$\begin{cases} v_{32}(\xi) = \frac{k_x^2}{24} - \frac{k_x^2 \cdot cosh(\xi) - 7 \cdot k_x^2}{8\left[\sqrt{cosh(\xi)+1}+r\right]^2} \\ \xi = k_x \cdot x + k_y \cdot y + \left(k_y^2 + \frac{k_x^4}{4}\right)/k_x \cdot t \end{cases} \text{and} \begin{cases} w_{32}(\xi) = \frac{k_x^2}{8} - \frac{k_x^2 \cdot cosh(\xi) - 7 \cdot k_x^2}{8\left[\sqrt{cosh(\xi)+1}+r\right]^2} \\ \xi = k_x \cdot x + k_y \cdot y + \left(k_y^2 - \frac{k_x^4}{4}\right)/k_x \cdot t \end{cases} \quad (57)$$

When $n = 3$, the solutions are shown as Equation (58), in which $r = \pm 4\sqrt[4]{2}$. The corresponding solitary wave evolution is shown as Figure 10 with $k_x = 1$, $k_y = 1$ and $y = 0$.

$$\begin{cases} v_{33}(\xi) = \frac{k_x^2}{96} - \frac{k_x^2 \cdot \sqrt{cosh(\xi)+1} - 15\sqrt{2} \cdot k_x^2}{32 \cdot \left[\sqrt{\sqrt{cosh(\xi)+1}+2\sqrt{2}}+r\right]^2} \\ \xi = k_x \cdot x + k_y \cdot y + \left(k_y^2 + \frac{k_x^4}{16}\right)/k_x \cdot t \end{cases} \text{and} \begin{cases} w_{33}(\xi) = \frac{k_x^2}{32} - \frac{k_x^2 \cdot \sqrt{cosh(\xi)+1} - 15\sqrt{2} \cdot k_x^2}{32 \cdot \left[\sqrt{\sqrt{cosh(\xi)+1}+2\sqrt{2}}+r\right]^2} \\ \xi = k_x \cdot x + k_y \cdot y + \left(k_y^2 - \frac{k_x^4}{16}\right)/k_x \cdot t \end{cases} \quad (58)$$

When $n = 4$, the solutions are shown as Equation (59), in which $r = \pm 4\sqrt{2\sqrt[4]{2}}$. The corresponding solitary wave evolution is shown as Figure 11 with $k_x = 1$, $k_y = 1$ and $y = 0$.

$$\begin{cases} v_{34}(\xi) = \frac{k_x^2}{384} - \frac{k_x^2 \cdot \sqrt{\sqrt{cosh(\xi)+1}+2\sqrt{2}} - 7\sqrt[4]{2} \cdot k_x^2}{128 \cdot \left[\sqrt{\sqrt{\sqrt{cosh(\xi)+1}+2\sqrt{2}}+4\sqrt[4]{2}}+r\right]^2} \\ \xi = k_x \cdot x + k_y \cdot y + \left(k_y^2 + \frac{k_x^4}{64}\right)/k_x \cdot t \end{cases} \text{and} \begin{cases} w_{34}(\xi) = \frac{k_x^2}{128} - \frac{k_x^2 \cdot \sqrt{\sqrt{cosh(\xi)+1}+2\sqrt{2}} - 7\sqrt[4]{2} \cdot k_x^2}{128 \cdot \left[\sqrt{\sqrt{\sqrt{cosh(\xi)+1}+2\sqrt{2}}+4\sqrt[4]{2}}+r\right]^2} \\ \xi = k_x \cdot x + k_y \cdot y + \left(k_y^2 - \frac{k_x^4}{64}\right)/k_x \cdot t \end{cases} \quad (59)$$

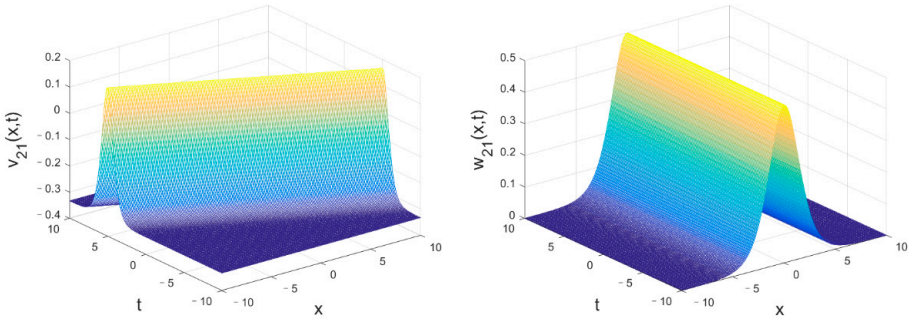

Figure 5. Bright solitary wave evolution of $v_{21}(\xi)$ (**left figure**) and $w_{21}(\xi)$ (**right figure**) vs. (x, t) when $k_x = 1$, $k_y = 1$, $r = 1$ and $y = 0$.

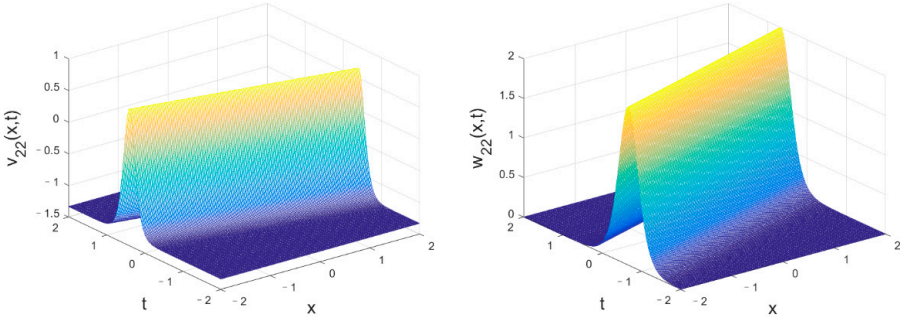

Figure 6. Bright solitary wave evolution of $v_{22}(\xi)$ (**left figure**) and $w_{22}(\xi)$ (**right figure**) vs. (x, t) when $k_x = 1$, $k_y = 1$, $r = 1$ and $y = 0$.

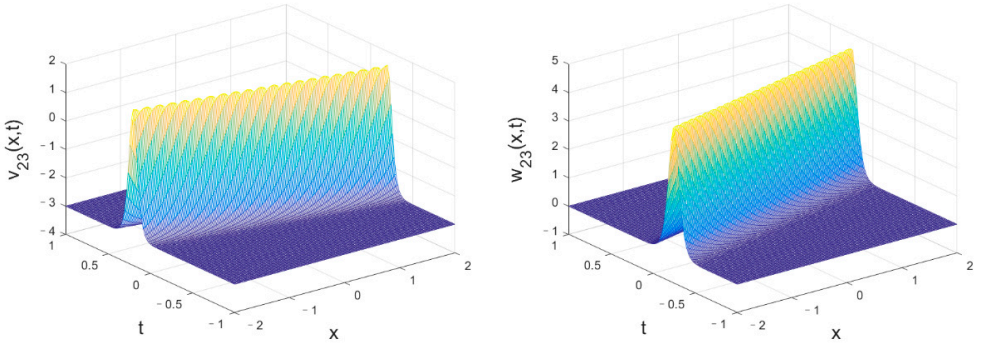

Figure 7. Bright solitary wave evolution of $v_{23}(\xi)$ (**left figure**) and $w_{23}(\xi)$ (**right figure**) vs. (x,t) when $k_x = 1, k_y = 1, r = 1$ and $y = 0$.

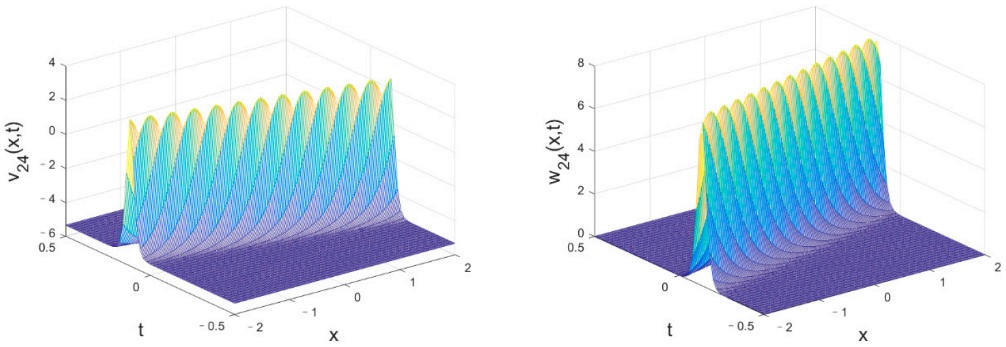

Figure 8. Bright solitary wave evolution of $v_{24}(\xi)$ (**left figure**) and $w_{24}(\xi)$ (**right figure**) vs. (x,t) when $k_x = 1, k_y = 1, r = 1$ and $y = 0$.

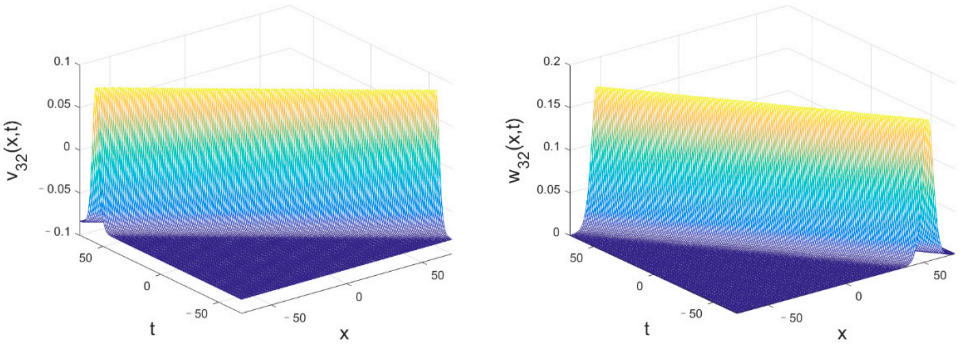

Figure 9. Bright solitary wave evolution of $v_{32}(\xi)$ (**left figure**) and $w_{32}(\xi)$ (**right figure**) vs. (x,t) when $k_x = 1, k_y = 1, r = \pm 2\sqrt{2}$ and $y = 0$.

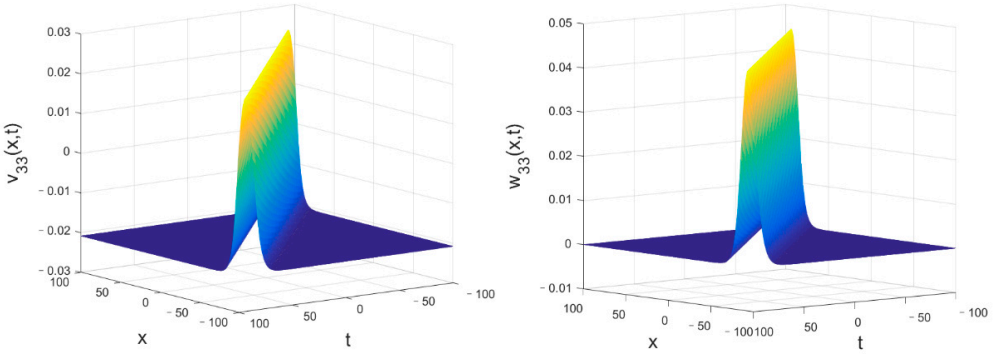

Figure 10. Bright solitary wave evolution of $v_{33}(\xi)$ (**left figure**) and $w_{33}(\xi)$ (**right figure**) vs. (x,t) when $k_x = 1, k_y = 1, r = \pm 4\sqrt[4]{2}$ and $y = 0$.

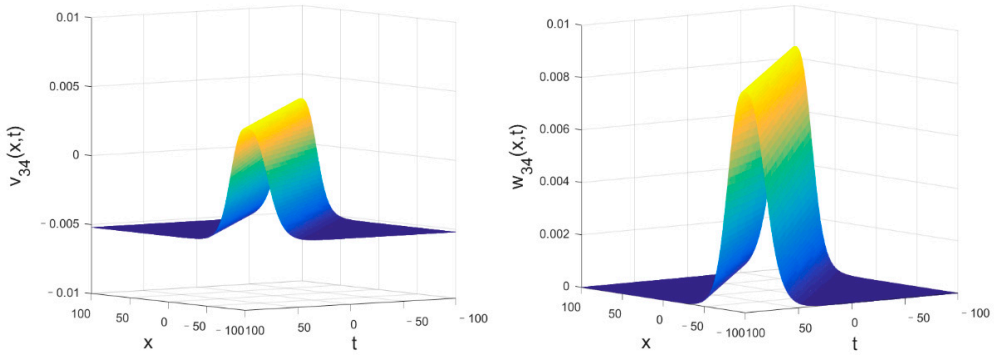

Figure 11. Bright solitary wave evolution of $v_{34}(\xi)$ (**left figure**) and $w_{34}(\xi)$ (**right figure**) vs. (x,t) when $k_x = 1$, $k_y = 1$, $r = \pm 4\sqrt{2\sqrt[4]{2}}$ and $y = 0$.

In this set of solutions, with the increase in n, the amplitude of the bright solitary wave decreases and the bandwidth in space–time increases. It would be easy to conclude that the solitary waves have relatively stable structures for different n.

4.4. The Fourth Set of Solutions

When $n = 1$, the solutions are shown as Equation (60). The corresponding solitary wave evolution is shown as Figure 12 with $k_x = 1$, $k_y = 1$ and $y = 0$.

$$\begin{cases} v_{41}(\xi) = \frac{2 \cdot k_x^2}{3} - \frac{2 \cdot k_x^2 \cdot cosh^2(\xi)}{sinh^2(\xi)} \\ \xi = k_x \cdot x + k_y \cdot y + \left(k_y^2 + 4k_x^4\right)/k_x \cdot t \end{cases} \text{and} \begin{cases} w_{41}(\xi) = 2 \cdot k_x^2 - \frac{2 \cdot k_x^2 \cdot cosh^2(\xi)}{sinh^2(\xi)} \\ \xi = k_x \cdot x + k_y \cdot y + \left(k_y^2 - 4k_x^4\right)/k_x \cdot t \end{cases} \quad (60)$$

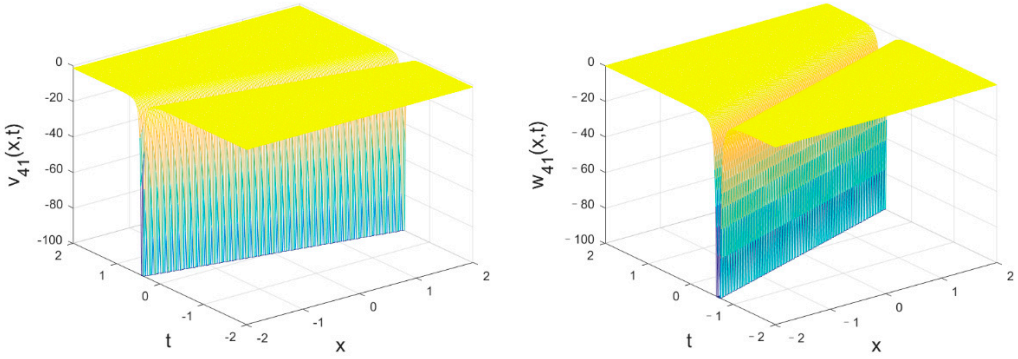

Figure 12. Dark solitary wave evolution of $v_{41}(\xi)$ (**left figure**) and $w_{41}(\xi)$ (**right figure**) vs. (x,t) when $k_x = 1$, $k_y = 1$ and $y = 0$.

When $n = 2$, the solutions are shown as Equation (61). The corresponding solitary wave evolution is shown as Figure 13 with $k_x = 1$, $k_y = 1$ and $y = 0$.

$$\begin{cases} v_{42}(\xi) = \frac{8 \cdot k_x^2}{3} - \frac{32 \cdot k_x^2 \cdot \left[cosh^2(\xi) - \frac{1}{2}\right]^2}{4\left[cosh^2(\xi) - \frac{1}{2}\right]^2 - 1} \\ \xi = k_x \cdot x + k_y \cdot y + \left(k_y^2 + 16k_x^4\right)/k_x \cdot t \end{cases} \text{and} \begin{cases} w_{42}(\xi) = 8 \cdot k_x^2 - \frac{32 \cdot k_x^2 \cdot \left[cosh^2(\xi) - \frac{1}{2}\right]^2}{4\left[cosh^2(\xi) - \frac{1}{2}\right]^2 - 1} \\ \xi = k_x \cdot x + k_y \cdot y + \left(k_y^2 - 16k_x^4\right)/k_x \cdot t \end{cases} \quad (61)$$

When $n = 3$, the solutions are shown as Equation (62). The corresponding solitary wave evolution is shown as Figure 14 with $k_x = 1$, $k_y = 1$ and $y = 0$.

$$\begin{cases} v_{43}(\xi) = \frac{32k_x^2}{3} - \frac{512k_x^2 \cdot \left[cosh^4(\xi) - cosh^2(\xi) + \frac{1}{8}\right]^2}{16\left[cosh^4(\xi) - cosh^2(\xi) + \frac{1}{8}\right]^2 - \frac{1}{4}} \\ \xi = k_x \cdot x + k_y \cdot y + \left(k_y^2 + 64k_x^4\right)/k_x \cdot t \end{cases} \text{and} \begin{cases} w_{43}(\xi) = 32k_x^2 - \frac{512k_x^2 \cdot \left[cosh^4(\xi) - cosh^2(\xi) + \frac{1}{8}\right]^2}{16\left[cosh^4(\xi) - cosh^2(\xi) + \frac{1}{8}\right]^2 - \frac{1}{4}} \\ \xi = k_x \cdot x + k_y \cdot y + \left(k_y^2 - 64k_x^4\right)/k_x \cdot t \end{cases} \quad (62)$$

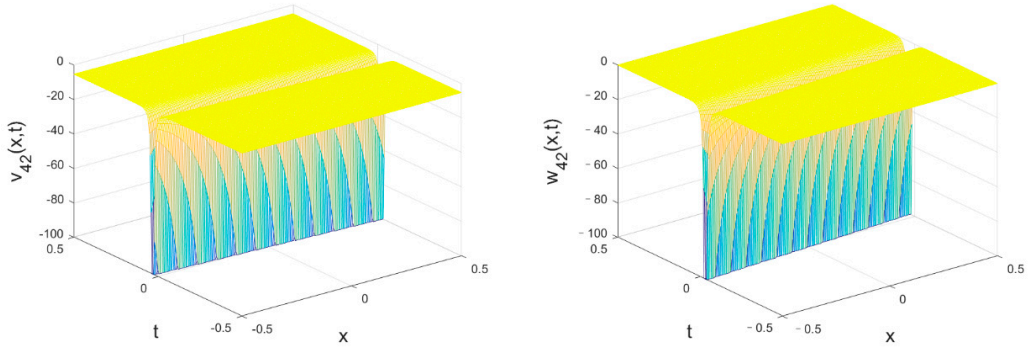

Figure 13. Dark solitary wave evolution of $v_{42}(\xi)$ (**left figure**) and $w_{42}(\xi)$ (**right figure**) vs. (x,t) when $k_x = 1$, $k_y = 1$ and $y = 0$.

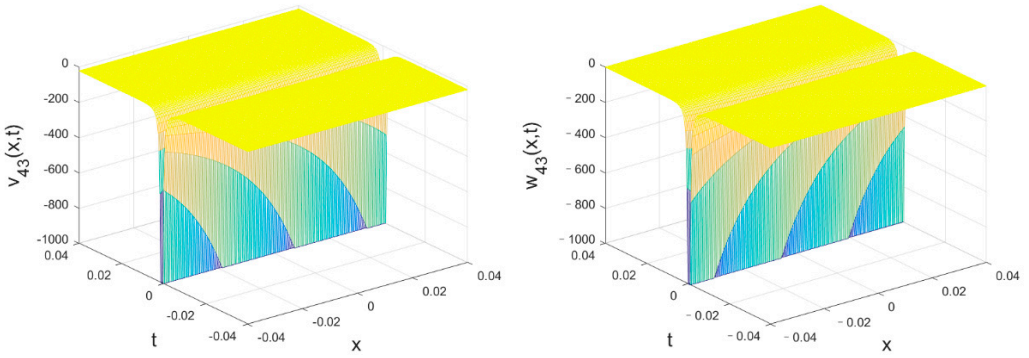

Figure 14. Dark solitary wave evolution of $v_{43}(\xi)$ (**left figure**) and $w_{43}(\xi)$ (**right figure**) vs. (x,t) when $k_x = 1$, $k_y = 1$ and $y = 0$.

When $n = 4$, the solutions are shown as Equation (63). The corresponding solitary wave evolution is shown as Figure 15 with $k_x = 1$, $k_y = 1$ and $y = 0$.

$$\begin{cases} v_{44}(\xi) = \frac{128\cdot k_x^2}{3} - \frac{8192\cdot k_x^2\cdot\left[cosh^8(\xi)-2cosh^6(\xi)+\frac{5}{4}cosh^4(\xi)-\frac{1}{4}cosh^2(\xi)-\frac{7}{64}\right]^2}{64\left[cosh^8(\xi)-2cosh^6(\xi)+\frac{5}{4}cosh^4(\xi)-\frac{1}{4}cosh^2(\xi)-\frac{7}{64}\right]^2-\frac{1}{256}} \\ \xi = k_x\cdot x + k_y\cdot y + \left(k_y^2 + 256k_x^4\right)/k_x\cdot t \end{cases} \text{ and}$$
$$\begin{cases} w_{44}(\xi) = 128\cdot k_x^2 - \frac{8192\cdot k_x^2\cdot\left[cosh^8(\xi)-2cosh^6(\xi)+\frac{5}{4}cosh^4(\xi)-\frac{1}{4}cosh^2(\xi)-\frac{7}{64}\right]^2}{64\left[cosh^8(\xi)-2cosh^6(\xi)+\frac{5}{4}cosh^4(\xi)-\frac{1}{4}cosh^2(\xi)-\frac{7}{64}\right]^2-\frac{1}{256}} \\ \xi = k_x\cdot x + k_y\cdot y + \left(k_y^2 - 256k_x^4\right)/k_x\cdot t \end{cases} \quad (63)$$

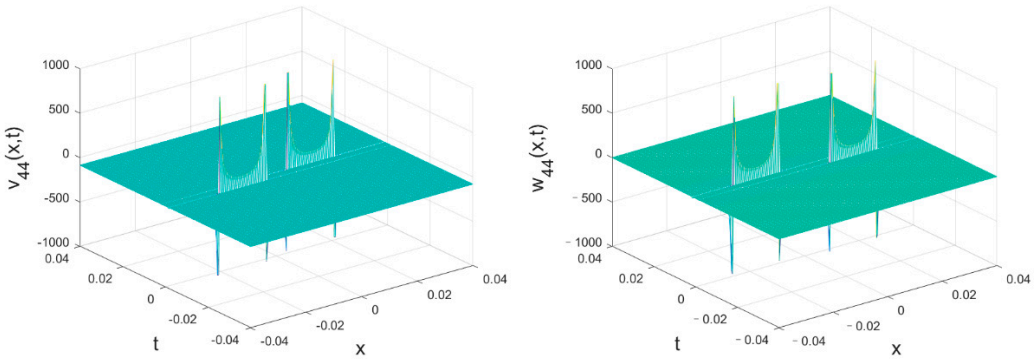

Figure 15. Solitary wave evolution of $v_{44}(\xi)$ (**left figure**) and $w_{44}(\xi)$ (**right figure**) vs. (x,t) when $k_x = 1$, $k_y = 1$ and $y = 0$.

Figures 12–15 show the dark solitary wave evolution for $n = 1$ to 4, respectively. The space–time width of the solitary wave decreases with the increase in n. However, under

certain conditions, this set of infinite solutions has singularities in some specific space–time positions, which makes the solitary wave structure unstable.

4.5. The Fifth Set of Solutions

According to $f_{5n}(\xi)$ given by Equation (37), the second set of solution $u_{5n}(\xi)$ is given by Equation (64):

$$\begin{cases} u_{5n}(\xi) = \frac{(-2\pm 2)}{3}\nu^2 n^2 k_x^2 + 8\lambda k_x^2 \frac{\nu^2 n^2 [sinh(\xi)+\varepsilon\cdot cosh(\xi)]^{2\nu n}}{[sinh(\xi)+\varepsilon\cdot cosh(\xi)]^{2\nu n}+r} - 8k_x^2 \left\{ \frac{\nu n [sinh(\xi)+\varepsilon\cdot cosh(\xi)]^{2\nu n}}{[sinh(\xi)+\varepsilon\cdot cosh(\xi)]^{2\nu n}+r} \right\}^2 \\ \left(\xi = k_x x + k_y y + ct, c = \left(k_y^2 \mp 4\nu^2 n^2 k_x^4\right)/k_x, \lambda^2 = 1, \varepsilon^2 = 1 \right) \end{cases} \tag{64}$$

Here, we only consider the case of $\lambda = 1$, $\nu = 1$, $\varepsilon = 1$ and $r = 1$. The expressions of $v(\xi)$ and $w(\xi)$ are shown as Equation (65):

$$\begin{cases} v_{5n}(\xi) = -\frac{4}{3}n^2 k_x^2 + 8k_x^2 \frac{n^2 [sinh(\xi)+cosh(\xi)]^{2n}}{[sinh(\xi)+cosh(\xi)]^{2n}+1} - 8k_x^2 \left\{ \frac{n[sinh(\xi)+cosh(\xi)]^{2n}}{[sinh(\xi)+cosh(\xi)]^{2n}+1} \right\}^2 \\ \xi = k_x \cdot x + k_y \cdot y + \left(k_y^2 + 4n^2 k_x^4\right)/k_x \cdot t \end{cases} \text{ and}$$
$$\begin{cases} w_{5n}(\xi) = 8k_x^2 \frac{n^2 [sinh(\xi)+cosh(\xi)]^{2n}}{[sinh(\xi)+cosh(\xi)]^{2n}+1} - 8k_x^2 \left\{ \frac{n[sinh(\xi)+cosh(\xi)]^{2n}}{[sinh(\xi)+cosh(\xi)]^{2n}+1} \right\}^2 \\ \xi = k_x \cdot x + k_y \cdot y + \left(k_y^2 - 4n^2 k_x^4\right)/k_x \cdot t \end{cases} \tag{65}$$

Respectively, Figures 16–19 show the dark solitary wave evolution for $n = 1$ to 4, when $k_x = 1$, $k_y = 1$ and $y = 0$. While n increases, the amplitude of the solitary wave increases, and the bandwidth decreases.

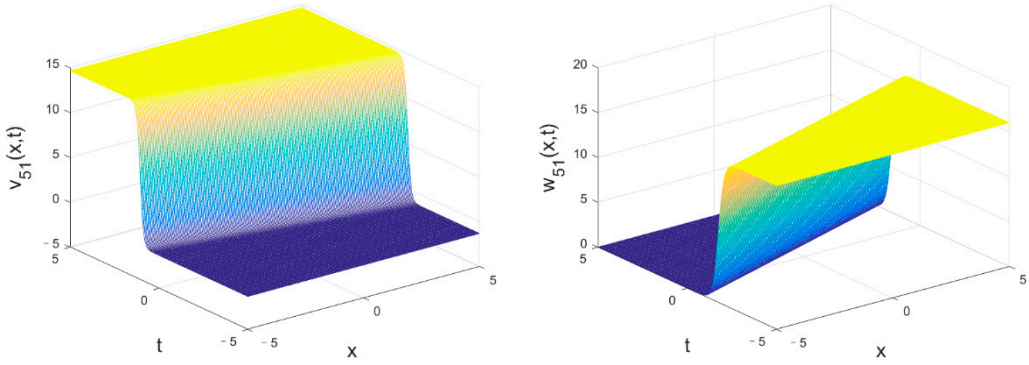

Figure 16. Wave evolution of $v_{51}(\xi)$ (**left figure**) and $w_{51}(\xi)$ (**right figure**) vs. (x, t) when $k_x = 1$, $k_y = 1$ and $y = 0$.

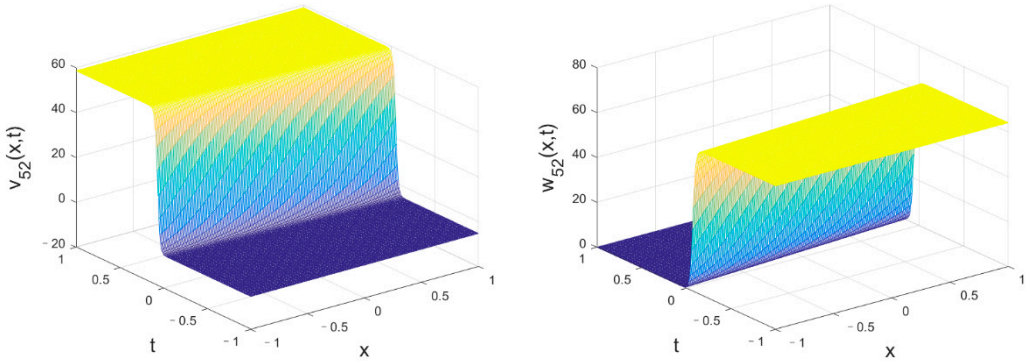

Figure 17. Wave evolution of $v_{52}(\xi)$ (**left figure**) and $w_{52}(\xi)$ (**right figure**) vs. (x, t) when $k_x = 1$, $k_y = 1$ and $y = 0$.

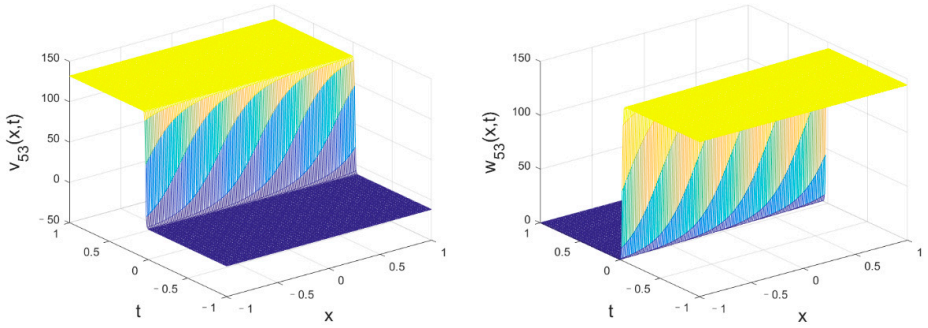

Figure 18. Wave evolution of $v_{53}(\xi)$ (**left figure**) and $w_{53}(\xi)$ (**right figure**) vs. (x,t) when $k_x = 1$, $k_y = 1$ and $y = 0$.

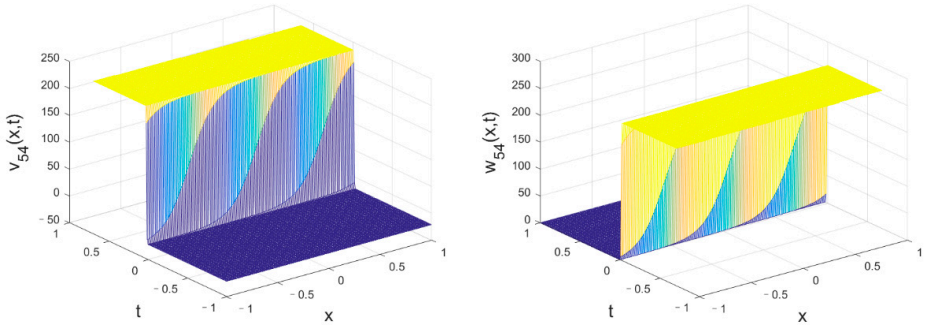

Figure 19. Wave evolution of $v_{54}(\xi)$ (**left figure**) and $w_{54}(\xi)$ (**right figure**) vs. (x,t) when $k_x = 1$, $k_y = 1$ and $y = 0$.

4.6. The Sixth Set of Solutions

Here, we only give the cases of $n \leq 4$ for $u_{6n}(\xi)$ for Equation (3). When $n = 1$, the solutions are shown as Equation (66), in which $r = \pm 1$. The corresponding solitary wave evolution is shown as Figure 20 with $k_x = 1$, $k_y = 1$ and $y = 0$.

$$\begin{cases} v_{61}(\xi) = \frac{k_x^2}{6} - \frac{k_x^2 \cdot [cosh(\xi)+r]^2}{2 \cdot sinh^2(\xi)} \\ \xi = k_x \cdot x + k_y \cdot y + \left(k_y^2 + k_x^4\right)/k_x \cdot t \end{cases} \text{ and } \begin{cases} w_{61}(\xi) = \frac{k_x^2}{2} - \frac{k_x^2 \cdot [cosh(\xi)+r]^2}{2 \cdot sinh^2(\xi)} \\ \xi = k_x \cdot x + k_y \cdot y + \left(k_y^2 - k_x^4\right)/k_x \cdot t \end{cases} \tag{66}$$

When $n = 2$, the solutions are shown as Equation (67), in which $r = \pm\frac{1}{2}$. The corresponding solitary wave evolution is shown as Figure 21 with $k_x = 1$, $k_y = 1$ and $y = 0$.

$$\begin{cases} v_{62}(\xi) = \frac{2k_x^2}{3} - \frac{8k_x^2 \cdot \left[cosh^2(\xi) - \frac{1}{2} + r\right]^2}{4\left[cosh^2(\xi) - \frac{1}{2}\right]^2 - 1} \\ \xi = k_x \cdot x + k_y \cdot y + \left(k_y^2 + 4k_x^4\right)/k_x \cdot t \end{cases} \text{ and } \begin{cases} w_{62}(\xi) = 2k_x^2 - \frac{8k_x^2 \cdot \left[cosh^2(\xi) - \frac{1}{2} + r\right]^2}{4\left[cosh^2(\xi) - \frac{1}{2}\right]^2 - 1} \\ \xi = k_x \cdot x + k_y \cdot y + \left(k_y^2 - 4k_x^4\right)/k_x \cdot t \end{cases} \tag{67}$$

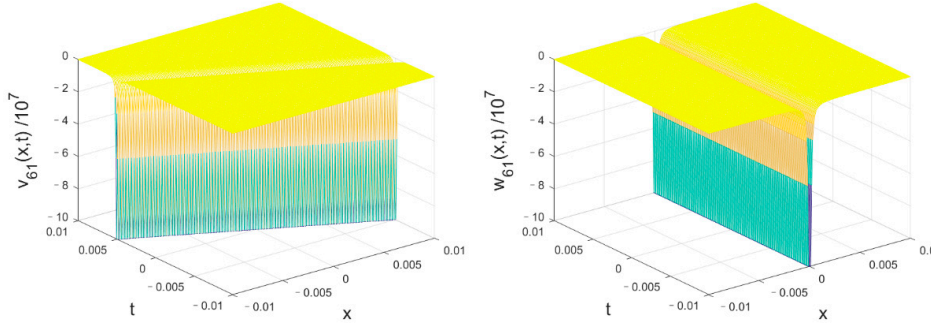

Figure 20. Dark solitary wave evolution of $v_{61}(\xi)$ (**left figure**) and $w_{61}(\xi)$ (**right figure**) vs. (x,t) when $k_x = 1$, $k_y = 1$, $r = 1$ and $y = 0$.

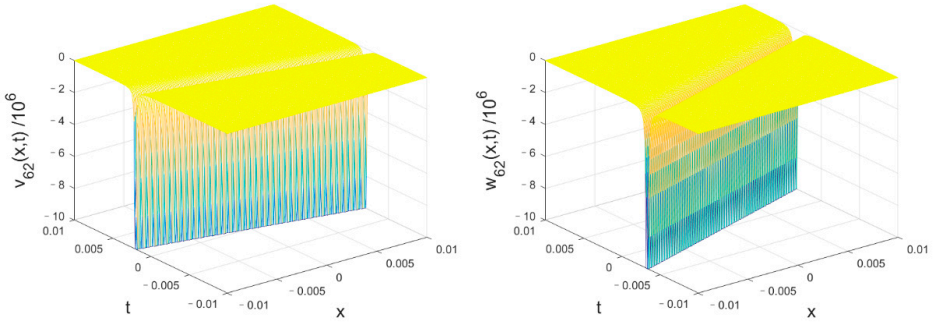

Figure 21. Dark solitary wave evolution of $v_{62}(\xi)$ (**left figure**) and $w_{62}(\xi)$ (**right figure**) vs. (x,t) when $k_x = 1, k_y = 1, r = 1/2$ and $y = 0$.

When $n = 3$, the solutions are shown as Equation (68), in which $r = \pm\frac{1}{8}$. The corresponding solitary wave evolution is shown as Figure 22 with $k_x = 1$, $k_y = 1$ and $y = 0$.

$$\begin{cases} v_{63}(\xi) = \frac{8k_x^2}{3} - \frac{128\cdot k_x^2\cdot\left[cosh^4(\xi)-cosh^2(\xi)+\frac{1}{8}+r\right]^2}{4cosh^8(\xi)-8cosh^6(\xi)+5cosh^4(\xi)-cosh^2(\xi)} \\ \xi = k_x\cdot x + k_y\cdot y + \left(k_y^2 + 16k_x^4\right)/k_x\cdot t \end{cases} \text{ and } \begin{cases} w_{63}(\xi) = 8k_x^2 - \frac{128\cdot k_x^2\cdot\left[cosh^4(\xi)-cosh^2(\xi)+\frac{1}{8}+r\right]^2}{4cosh^8(\xi)-8cosh^6(\xi)+5cosh^4(\xi)-cosh^2(\xi)} \\ \xi = k_x\cdot x + k_y\cdot y + \left(k_y^2 - 16k_x^4\right)/k_x\cdot t \end{cases} \quad (68)$$

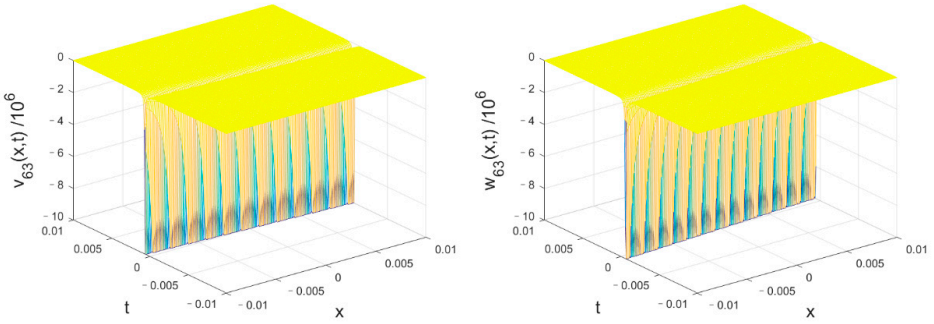

Figure 22. Dark solitary wave evolution of $v_{63}(\xi)$ (**left figure**) and $w_{63}(\xi)$ (**right figure**) vs. (x,t) when $k_x = 1, k_y = 1, r = 1/8$ and $y = 0$.

When $n = 4$, the solutions are shown as Equation (69), in which $r = \pm\frac{1}{128}$. The corresponding solitary wave evolution is shown as Figure 23 with $k_x = 1$, $k_y = 1$ and $y = 0$.

$$\begin{cases} v_{64}(\xi) = \frac{32\cdot k_x^2}{3} - \frac{2048\cdot k_x^2\cdot\left[cosh^8(\xi)-2cosh^6(\xi)+\frac{5}{4}cosh^4(\xi)-\frac{1}{4}cosh^2(\xi)-\frac{7}{64}+r\right]^2}{64\cdot\left[cosh^8(\xi)-2cosh^6(\xi)+\frac{5}{4}cosh^4(\xi)-\frac{1}{4}cosh^2(\xi)-\frac{7}{64}\right]^2-\frac{1}{256}} \\ \xi = k_x\cdot x + k_y\cdot y + \left(k_y^2 + 64k_x^4\right)/k_x\cdot t \end{cases} \text{ and}$$
$$\begin{cases} w_{64}(\xi) = 32\cdot k_x^2 - \frac{2048\cdot k_x^2\cdot\left[cosh^8(\xi)-2cosh^6(\xi)+\frac{5}{4}cosh^4(\xi)-\frac{1}{4}cosh^2(\xi)-\frac{7}{64}+r\right]^2}{64\cdot\left[cosh^8(\xi)-2cosh^6(\xi)+\frac{5}{4}cosh^4(\xi)-\frac{1}{4}cosh^2(\xi)-\frac{7}{64}\right]^2-\frac{1}{256}} \\ \xi = k_x\cdot x + k_y\cdot y + \left(k_y^2 - 64k_x^4\right)/k_x\cdot t \end{cases} \quad (69)$$

Figures 20–22 represent the dark solitary wave solutions of the KPI equation. Due to the existence of singularities, the solitary wave structure of each solution is completely unstable.

4.7. The Seventh Set of Solutions

According to $f_{7n}(\xi)$ given by Equation (39), the seventh set of solution $u_{7n}(\xi)$ is given by Equation (70).

$$\begin{cases} u_{7n}(\xi) = \left(\frac{1}{3} \pm \frac{1}{6}\right)\nu^2 n^2 k^2 - 2k^2\left\{\frac{\nu n[sinh(\xi)+\varepsilon\cdot cosh(\xi)]^{\nu n}+\nu nr}{(2\lambda+4\varepsilon)[sinh(\xi)+\varepsilon\cdot cosh(\xi)]^{\nu n}+2\lambda r}\right\}^2 \\ \left(\ \xi = k_x x + k_y y + ct, c = \left(k_y^2 \mp \nu^2 n^2 k_x^4\right)/k_x, \lambda^2 = 1, \varepsilon^2 = 1.\ \right) \end{cases} \quad (70)$$

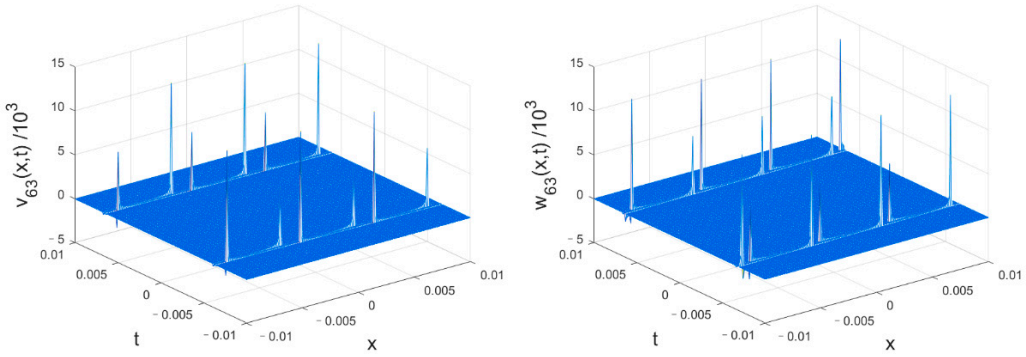

Figure 23. Solitary wave evolution of $v_{64}(\xi)$ (**left figure**) and $w_{64}(\xi)$ (**right figure**) vs. (x,t) when $k_x = 1$, $k_y = 1$, $r = 1/128$ and $y = 0$.

Here, we only consider the case of $\lambda = 1$, $\nu = 1$, $\varepsilon = 1$ and $r = 1$. The expressions of $v(\xi)$ and $w(\xi)$ are shown as Equation (71).

$$\begin{cases} v_{7n}(\xi) = \frac{n^2k_x^2}{6} - 2k_x^2\left\{\frac{n[sinh(\xi)+cosh(\xi)]^n+n}{6\cdot[sinh(\xi)+cosh(\xi)]^n+2}\right\}^2 \\ \xi = k_x\cdot x + k_y\cdot y + \left(k_y^2 + n^2k_x^4\right)/k_x\cdot t \end{cases} \text{ and } \begin{cases} w_{7n}(\xi) = \frac{n^2k_x^2}{2} - 2k_x^2\left\{\frac{n[sinh(\xi)+cosh(\xi)]^n+n}{6\cdot[sinh(\xi)+cosh(\xi)]^n+2}\right\}^2 \\ \xi = k_x\cdot x + k_y\cdot y + \left(k_y^2 - n^2k_x^4\right)/k_x\cdot t \end{cases} \quad (71)$$

The solutions of $n = 1$ to 4 are shown as Figures 24–27, respectively. We find that the structures of these solutions have an abrupt change in their amplitude, which maybe implies a bistable mode, including those with fractional derivatives [45], which is of particular interest in optical technology, power networks, and so on [46,47]. Different values of n can make the amplitude, space–time width, kink direction, and singularity position of the solitary wave different. In this case, all the solitary waves have relatively stable structures.

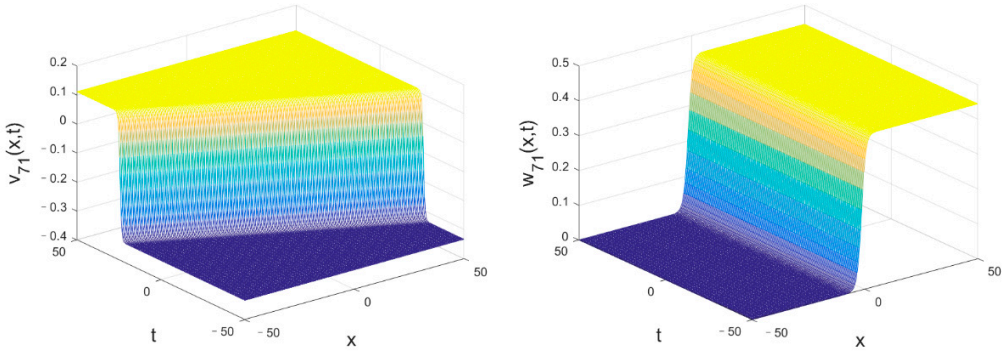

Figure 24. Wave evolution of $v_{71}(\xi)$ (**left figure**) and $w_{71}(\xi)$ (**right figure**) vs. (x,t) when $k_x = 1$, $k_y = 1$ and $y = 0$.

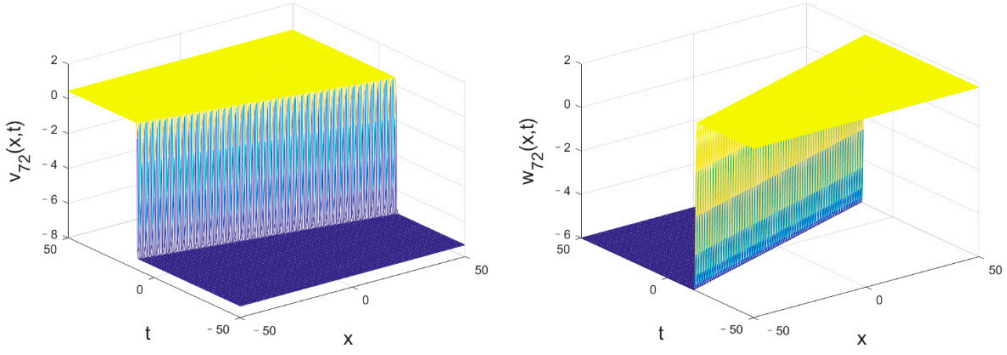

Figure 25. Wave evolution of $v_{72}(\xi)$ (**left figure**) and $w_{72}(\xi)$ (**right figure**) vs. (x,t) when $k_x = 1$, $k_y = 1$ and $y = 0$.

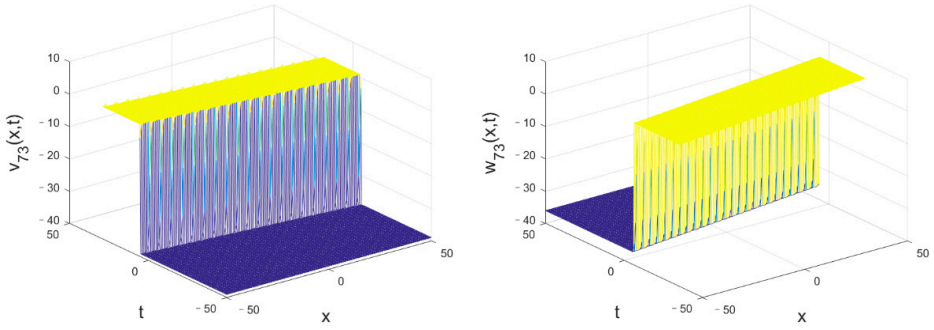

Figure 26. Wave evolution of $v_{73}(\xi)$ (**left figure**) and $w_{73}(\xi)$ (**right figure**) vs. (x,t) when $k_x = 1$, $k_y = 1$ and $y = 0$.

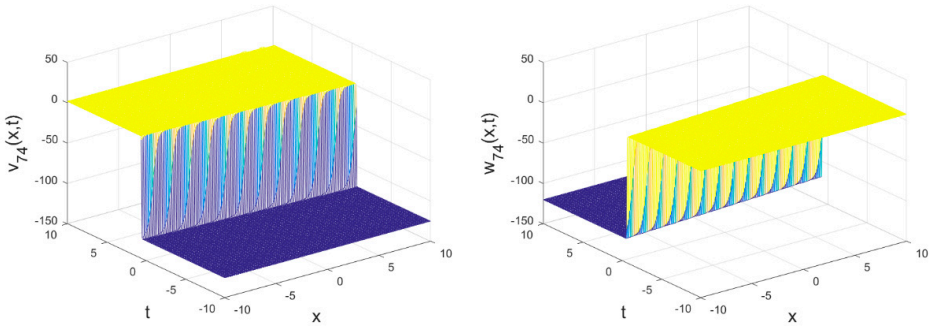

Figure 27. Wave evolution of $v_{74}(\xi)$ (**left figure**) and $w_{74}(\xi)$ (**right figure**) vs. (x,t) when $k_x = 1$, $k_y = 1$ and $y = 0$.

4.8. The Eighth Set of Solutions

The cases of $n \leq 4$ for $u_{8n}(\xi)$ for Equation (3) is given below. When $n = 1$, the solutions are shown as Equation (72), in which $r = \pm 1$. These solutions are to the same as v_{61} and w_{61} given in Section 4.6, which will not be repeated here.

$$\begin{cases} v_{81}(\xi) = \frac{k_x^2}{6} - \frac{k_x^2 \cdot [cosh(\xi)+r]^2}{2 \cdot sinh^2(\xi)} \\ \xi = k_x \cdot x + k_y \cdot y + \left(k_y^2 + k_x^4\right)/k_x \cdot t \end{cases} \text{ and } \begin{cases} w_{81}(\xi) = \frac{k_x^2}{2} - \frac{k_x^2 \cdot [cosh(\xi)+r]^2}{2 \cdot sinh^2(\xi)} \\ \xi = k_x \cdot x + k_y \cdot y + \left(k_y^2 - k_x^4\right)/k_x \cdot t \end{cases} \quad (72)$$

When $n = 2$, the solutions are shown as Equation (73), in which $r = \pm 2\sqrt{2}$. The corresponding solitary wave evolution is shown as Figure 28 with $k_x = 1$, $k_y = 1$ and $y = 0$.

$$\begin{cases} v_{82}(\xi) = \frac{k_x^2}{24} - \frac{k_x^2 \cdot \left[\sqrt{cosh(\xi)+1}+r\right]^2}{8 \cdot cosh(\xi) - 56} \\ \xi = k_x \cdot x + k_y \cdot y + \left(k_y^2 + \frac{k_x^4}{4}\right)/k_x \cdot t \end{cases} \text{ and } \begin{cases} w_{82}(\xi) = \frac{k_x^2}{8} - \frac{k_x^2 \cdot \left[\sqrt{cosh(\xi)+1}+r\right]^2}{8 \cdot cosh(\xi) - 56} \\ \xi = k_x \cdot x + k_y \cdot y + \left(k_y^2 - \frac{k_x^4}{4}\right)/k_x \cdot t \end{cases} \quad (73)$$

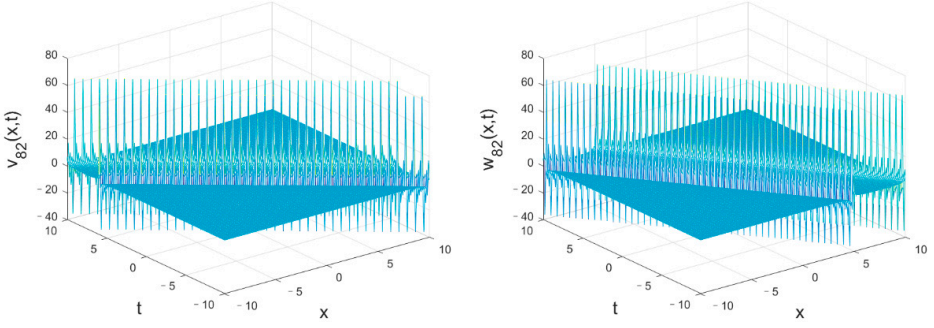

Figure 28. Solitary wave evolution of $v_{82}(\xi)$ (**left figure**) and $w_{82}(\xi)$ (**right figure**) vs. (x,t) when $k_x = 1$, $k_y = 1$, $r = 2\sqrt{2}$ and $y = 0$.

When $n = 3$, the solutions are shown as Equation (74), in which $r = \pm 4\sqrt[4]{2}$. The corresponding solitary wave evolution is shown as Figure 29 with $k_x = 1$, $k_y = 1$ and $y = 0$.

$$\begin{cases} v_{83}(\xi) = \frac{k_x^2}{96} - \frac{k_x^2 \cdot \left[\sqrt{\sqrt{cosh(\xi)+1}+2\sqrt{2}}+r\right]^2}{32 \cdot \sqrt{cosh(\xi)+1}-480\sqrt{2}} \\ \xi = k_x \cdot x + k_y \cdot y + \left(k_y^2 + \frac{k_x^4}{16}\right)/k_x \cdot t \end{cases} \text{ and } \begin{cases} w_{83}(\xi) = \frac{k_x^2}{32} - \frac{k_x^2 \cdot \left[\sqrt{\sqrt{cosh(\xi)+1}+2\sqrt{2}}+r\right]^2}{32 \cdot \sqrt{cosh(\xi)+1}-480\sqrt{2}} \\ \xi = k_x \cdot x + k_y \cdot y + \left(k_y^2 - \frac{k_x^4}{16}\right)/k_x \cdot t \end{cases} \quad (74)$$

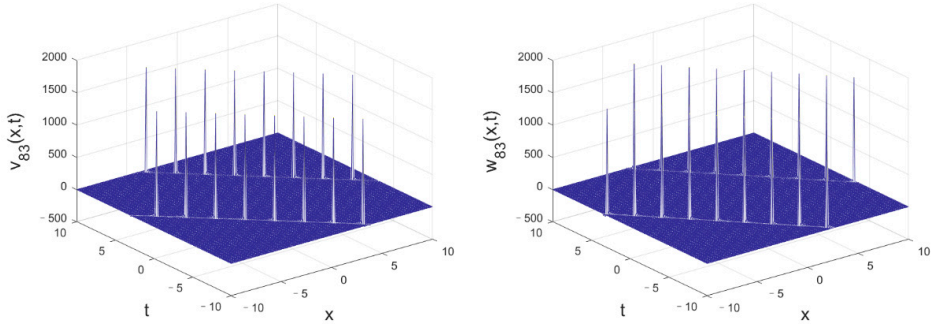

Figure 29. Solitary wave evolution of $v_{83}(\xi)$ (**left figure**) and $w_{83}(\xi)$ (**right figure**) vs. (x, t) when $k_x = 1$, $k_y = 1$, $r = 4\sqrt[4]{2}$ and $y = 0$.

When $n = 4$, the solutions are shown as Equation (75), in which $r = \pm 4\sqrt{2\sqrt[4]{2}}$. The corresponding solitary wave evolution is shown as Figure 30 with $k_x = 1$, $k_y = 1$ and $y = 0$.

$$\begin{cases} v_{84}(\xi) = \frac{k_x^2}{384} - \frac{k_x^2 \cdot \left[\sqrt{\sqrt{\sqrt{cosh(\xi)+1}+2\sqrt{2}}+4\sqrt[4]{2}}+r\right]^2}{128 \cdot \sqrt{\sqrt{cosh(\xi)+1}+2\sqrt{2}}-3584\sqrt[4]{2}} \\ \xi = k_x \cdot x + k_y \cdot y + \left(k_y^2 + \frac{k_x^4}{64}\right)/k_x \cdot t \end{cases} \text{ and } \begin{cases} w_{84}(\xi) = \frac{k_x^2}{128} - \frac{k_x^2 \cdot \left[\sqrt{\sqrt{\sqrt{cosh(\xi)+1}+2\sqrt{2}}+4\sqrt[4]{2}}+r\right]^2}{128 \cdot \sqrt{\sqrt{cosh(\xi)+1}+2\sqrt{2}}-3584\sqrt[4]{2}} \\ \xi = k_x \cdot x + k_y \cdot y + \left(k_y^2 - \frac{k_x^4}{64}\right)/k_x \cdot t \end{cases} \quad (75)$$

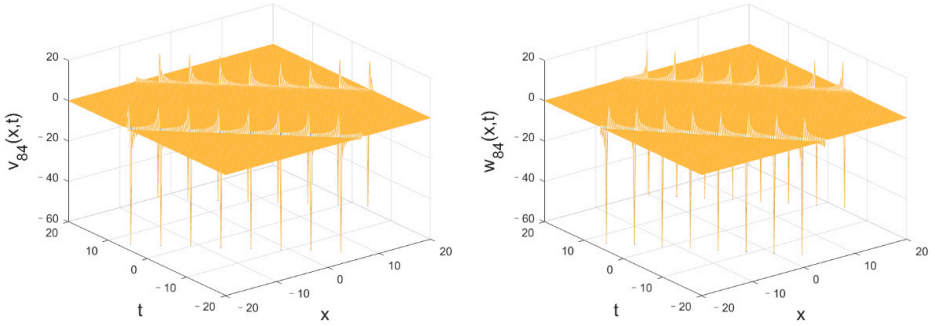

Figure 30. Solitary wave evolution of $v_{84}(\xi)$ (**left figure**) and $w_{84}(\xi)$ (**right figure**) vs. (x, t) when $k_x = 1$, $k_y = 1$, $r = 4\sqrt{2\sqrt[4]{2}}$ and $y = 0$.

It can be seen that the shape of the solitary wave and the space–time position of singular points will change with the value of n. $v_{81}(\xi)$ and $w_{81}(\xi)$ represent dark solitary waves. With the increase in n, it gradually evolves into a traveling wave with two rows of singular points. The solitary wave structure becomes unstable under high-n conditions.

4.9. The Ninth Set of Solutions

When $n = 1$, the solutions are shown as Equation (76). The corresponding solitary wave evolution is shown as Figure 31 with $k_x = 1$, $k_y = 1$ and $y = 0$.

$$\begin{cases} v_{91}(\xi) = \frac{2k_x^2}{3} - \frac{2k_x^2 \cdot sinh^2(\xi)}{cosh^2(\xi)} \\ \xi = k_x \cdot x + k_y \cdot y + \left(k_y^2 + 4k_x^4\right)/k_x \cdot t \end{cases} \text{ and } \begin{cases} w_{91}(\xi) = 2k_x^2 - \frac{2k_x^2 \cdot sinh^2(\xi)}{cosh^2(\xi)} \\ \xi = k_x \cdot x + k_y \cdot y + \left(k_y^2 - 4k_x^4\right)/k_x \cdot t \end{cases} \quad (76)$$

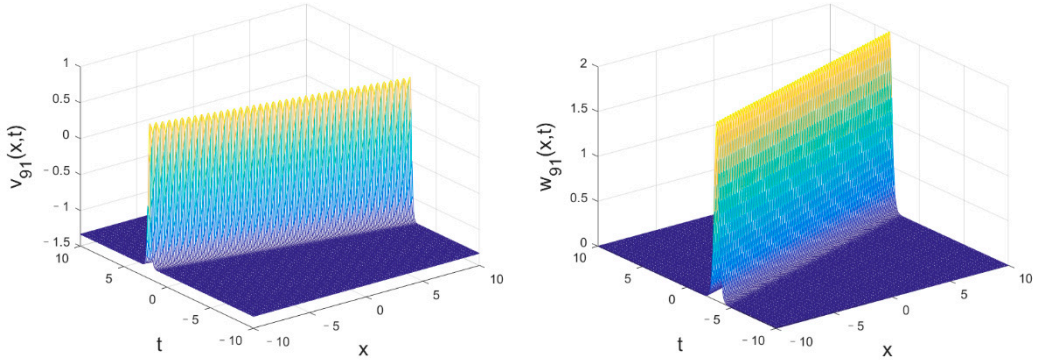

Figure 31. Wave evolution of $v_{91}(\xi)$ (**left figure**) and $w_{91}(\xi)$ (**right figure**) vs. (x,t) when $k_x = 1$, $k_y = 1$ and $y = 0$.

When $n = 2$, the solutions are shown as Equation (77). The corresponding solitary wave evolution is shown as Figure 32 with $k_x = 1$, $k_y = 1$ and $y = 0$.

$$\begin{cases} v_{92}(\xi) = \frac{8k_x^2}{3} - 2k_x^2 \cdot \frac{4\cdot\left[cosh^2(\xi)-\frac{1}{2}\right]^2-1}{\left[cosh^2(\xi)-\frac{1}{2}\right]^2} \\ \xi = k_x\cdot x + k_y\cdot y + \left(k_y^2 + 16k_x^4\right)/k_x\cdot t \end{cases} \text{ and } \begin{cases} w_{92}(\xi) = 8k_x^2 - 2k_x^2 \cdot \frac{4\cdot\left[cosh^2(\xi)-\frac{1}{2}\right]^2-1}{\left[cosh^2(\xi)-\frac{1}{2}\right]^2} \\ \xi = k_x\cdot x + k_y\cdot y + \left(k_y^2 - 16k_x^4\right)/k_x\cdot t \end{cases} \tag{77}$$

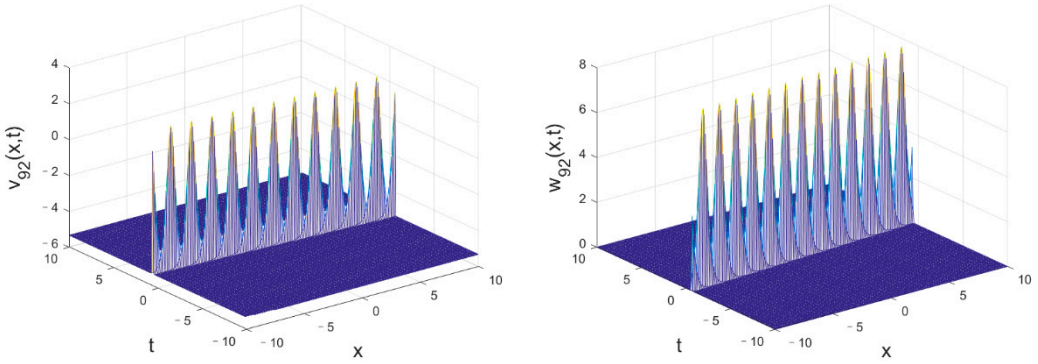

Figure 32. Wave evolution of $v_{92}(\xi)$ (**left figure**) and $w_{92}(\xi)$ (**right figure**) vs. (x,t) when $k_x = 1$, $k_y = 1$ and $y = 0$.

When $n = 3$, the solutions are shown as Equation (78). The corresponding solitary wave evolution is shown as Figure 33 with $k_x = 1$, $k_y = 1$ and $y = 0$.

$$\begin{cases} v_{93}(\xi) = \frac{32k_x^2}{3} - 2k_x^2 \frac{16\left\{\left[cosh^2(\xi)-\frac{1}{2}\right]^2-\frac{1}{8}\right\}^2-\frac{1}{4}}{\left\{\left[cosh^2(\xi)-\frac{1}{2}\right]^2-\frac{1}{8}\right\}^2} \\ \xi = k_x\cdot x + k_y\cdot y + \left(k_y^2 + 64k_x^4\right)/k_x\cdot t \end{cases} \text{and} \begin{cases} w_{93}(\xi) = 32k_x^2 - 2k_x^2 \frac{16\left\{\left[cosh^2(\xi)-\frac{1}{2}\right]^2-\frac{1}{8}\right\}^2-\frac{1}{4}}{\left\{\left[cosh^2(\xi)-\frac{1}{2}\right]^2-\frac{1}{8}\right\}^2} \\ \xi = k_x\cdot x + k_y\cdot y + \left(k_y^2 - 64k_x^4\right)/k_x\cdot t \end{cases} \tag{78}$$

When $n = 4$, the solutions are shown as Equation (79). The corresponding solitary wave evolution is shown as Figure 34 with $k_x = 1$, $k_y = 1$ and $y = 0$.

$$\begin{cases} v_{94}(\xi) = \frac{128k_x^2}{3} - 2k_x^2 \cdot \frac{64\left[cosh^8(\xi)-2cosh^6(\xi)+\frac{5}{4}cosh^4(\xi)-\frac{1}{4}cosh^2(\xi)-\frac{7}{64}\right]^2-\frac{1}{256}}{\left[cosh^8(\xi)-2cosh^6(\xi)+\frac{5}{4}cosh^4(\xi)-\frac{1}{4}cosh^2(\xi)-\frac{7}{64}\right]^2} \\ \xi = k_x\cdot x + k_y\cdot y + \left(k_y^2 + 256k_x^4\right)/k_x\cdot t \end{cases} \text{and}$$
$$\begin{cases} w_{94}(\xi) = 128k_x^2 - 2k_x^2 \cdot \frac{64\left[cosh^8(\xi)-2cosh^6(\xi)+\frac{5}{4}cosh^4(\xi)-\frac{1}{4}cosh^2(\xi)-\frac{7}{64}\right]^2-\frac{1}{256}}{\left[cosh^8(\xi)-2cosh^6(\xi)+\frac{5}{4}cosh^4(\xi)-\frac{1}{4}cosh^2(\xi)-\frac{7}{64}\right]^2} \\ \xi = k_x\cdot x + k_y\cdot y + \left(k_y^2 - 256k_x^4\right)/k_x\cdot t \end{cases} \tag{79}$$

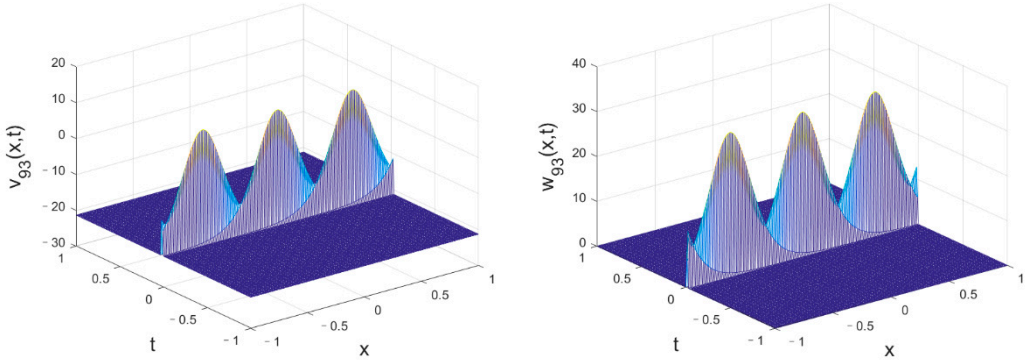

Figure 33. Wave evolution of $v_{93}(\xi)$ (**left figure**) and $w_{93}(\xi)$ (**right figure**) vs. (x,t) when $k_x = 1$, $k_y = 1$ and $y = 0$.

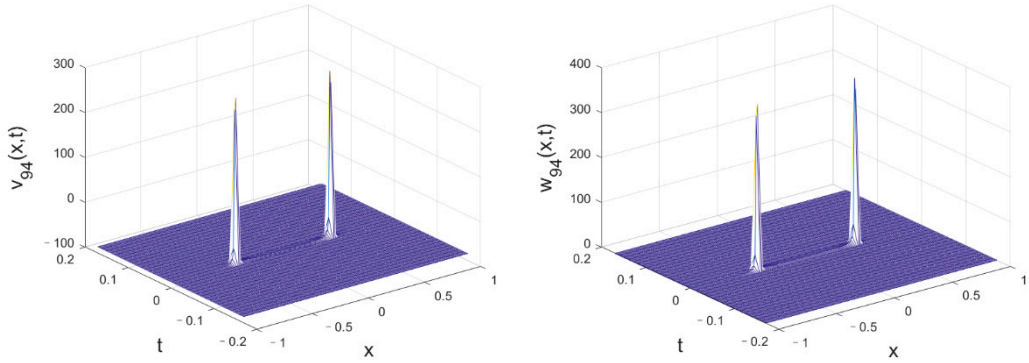

Figure 34. Wave evolution of $v_{94}(\xi)$ (**left figure**) and $w_{94}(\xi)$ (**right figure**) vs. (x,t) when $k_x = 1$, $k_y = 1$ and $y = 0$.

In this case, the increase in n reduces the space–time width of the solitary wave and changes the space–time position of the singularity. $v_{91}(\xi)$ and $w_{91}(\xi)$ represent bright solitary waves. With the increase in n, it gradually evolves into a traveling wave with many singular points. In this case, stable solitary wave structures only exist under low-n conditions, while they become unstable under high-n conditions.

4.10. The Tenth Set of Solutions

According to $f_{Xn}(\xi)$ given by Equation (42), the second set of solution $u_{Xn}(\xi)$ is given by Equation (80).

$$\begin{cases} u_{Xn}(\xi) = \left(\frac{4}{3} \pm \frac{2}{3}\right)\nu^2 n^2 k^2 - 2k^2 \left\{ \frac{\nu n[sinh(\xi)+\varepsilon\cdot cosh(\xi)]^{2\nu n}+\nu nr}{(\lambda-2\varepsilon)[sinh(\xi)+\varepsilon\cdot cosh(\xi)]^{2\nu n}\pm r} \right\}^2 \\ \left(\xi = k_x x + k_y y + ct, c = \left(k_y^2 \mp 4\nu^2 n^2 k_x^4\right)/k_x, \mu = -\frac{\nu^2\cdot n^2}{4}, \lambda^2 = 1, \varepsilon^2 = 1. \right) \end{cases} \tag{80}$$

Here, we only consider the cases of $\lambda = 1$, $\nu = 1$, $\varepsilon = 1$ and $r = 1$. The expressions of $v(\xi)$ and $w(\xi)$ are shown as Equation (81).

$$\begin{cases} v_{Xn}(\xi) = \frac{2}{3}n^2 k_x^2 - 2k^2 \left\{ \frac{n[sinh(\xi)+cosh(\xi)]^{2n}+n}{-[sinh(\xi)+cosh(\xi)]^{2n}+1} \right\}^2 \\ \xi = k_x\cdot x + k_y\cdot y + \left(k_y^2 + 4n^2 k_x^4\right)/k_x\cdot t \end{cases} \text{ and } \begin{cases} w_{Xn}(\xi) = 2n^2 k_x^2 - 2k^2 \left\{ \frac{n[sinh(\xi)+cosh(\xi)]^{2n}+n}{-[sinh(\xi)+cosh(\xi)]^{2n}+1} \right\}^2 \\ \xi = k_x\cdot x + k_y\cdot y + \left(k_y^2 - 4n^2 k_x^4\right)/k_x\cdot t \end{cases} \tag{81}$$

Figures 35–38 represent the 10th set of solitary wave solutions of the KPI equation. The increase in n can change the amplitude, space–time width, singularity position, and propagation direction of the solitary wave. In this case, under low-n conditions, there are very stable solitary wave structures, while under high-n conditions, the wave structures become unstable.

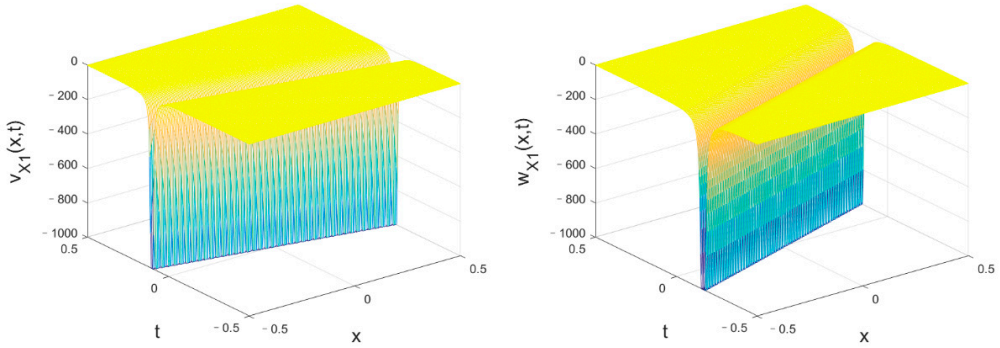

Figure 35. Wave evolution of $v_{X1}(\xi)$ (**left figure**) and $w_{X1}(\xi)$ (**right figure**) vs. (x,t) when $k_x = 1$, $k_y = 1$ and $y = 0$.

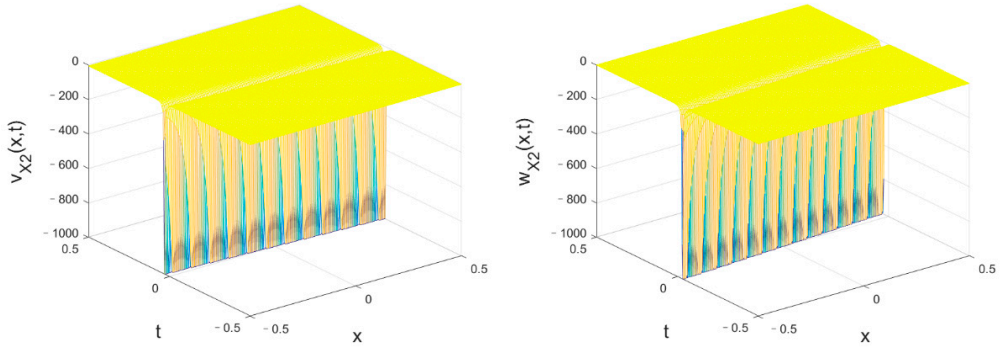

Figure 36. Wave evolution of $v_{X2}(\xi)$ (**left figure**) and $w_{X2}(\xi)$ (**right figure**) vs. (x,t) when $k_x = 1$, $k_y = 1$ and $y = 0$.

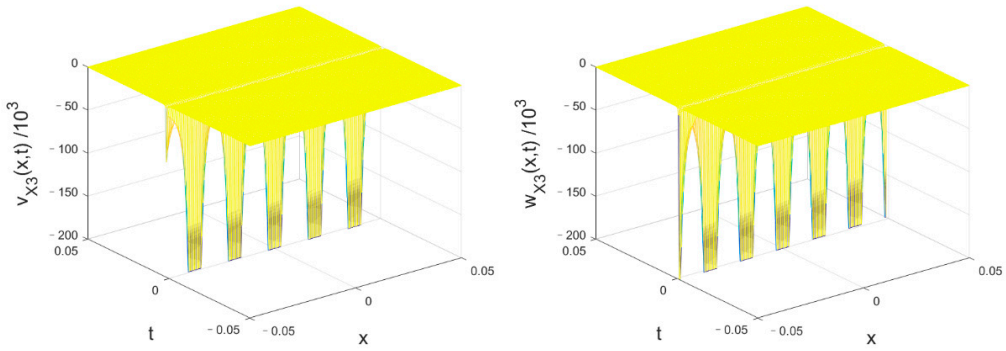

Figure 37. Wave evolution of $v_{X3}(\xi)$ (**left figure**) and $w_{X3}(\xi)$ (**right figure**) vs. (x,t) when $k_x = 1$, $k_y = 1$ and $y = 0$.

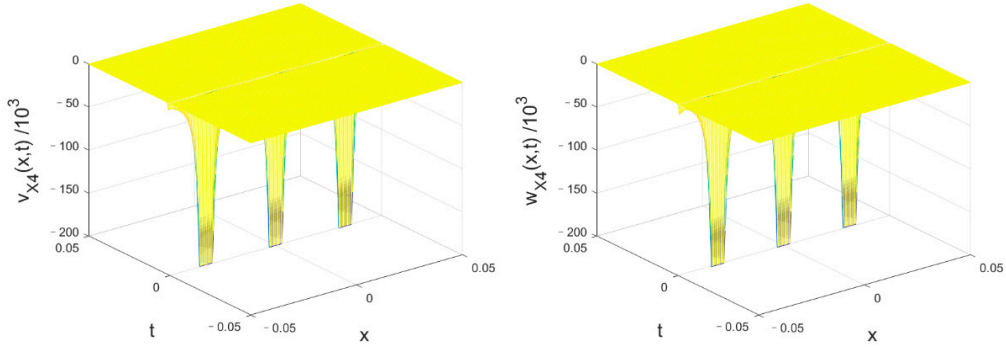

Figure 38. Wave evolution of $v_{X4}(\xi)$ (**left figure**) and $w_{X4}(\xi)$ (**right figure**) vs. (x,t) when $k_x = 1$, $k_y = 1$ and $y = 0$.

5. Summary

In nature, most nonlinear phenomena can be expressed as corresponding mathematical models under specific approximate conditions, and be simplified as NLEEs varying with time and space. In the study of such processes, the accuracy and stability of the solution is important. Many researchers have developed various methods to obtain the analytical solutions of NLEEs. The KPI equation is a well-known NLEE. In recent years, its applications in nonlinear optics, plasma ion acoustic mechanics, and other fields have made significant progress. Acquiring precise answers to the KPI equation is a crucial research tool in these fields.

In this paper, a general Riccati equation is treated as an auxiliary equation. Through different function transformations of $f(\xi)$ shown as Equation (13), (33) and $a_1/f(\xi)$, ten sets of infinite-series solitary wave solutions of the KPI equation have been constructed via the auxiliary equation method, which would be helpful to study the nonlinear problems described by the KPI equation. Unlike some other methods which can only provide a limited number of solutions, we can construct infinite-series exact solitary wave solutions with a relatively simple method.

The images of the first four solutions of each set have been plotted to provide intuitive structure of waves. Among these infinite-series exact wave solutions of the KPI equation, we find different structures of waves, including bright solitary waves, dark solitary waves, kink solitary waves and, traveling waves with singular points. Some of these solutions are stable, and the others are relatively unstable. A simple and intuitive introduction is given in Section 4. These results not only include known solutions, but also put forward some new forms of solutions, such as kink mode and traveling wave with many singular points, which may imply a new evolution mode. The detailed analysis should be combined with specific research objects, which will be discussed in future research papers. The results show that this method is simple and effective for the construction of infinite series solutions of nonlinear evolution models.

Author Contributions: Conceptualization, G.W. and Y.G.; methodology, G.W.; software, F.P.; validation, G.W. and Y.G.; formal analysis, F.P.; investigation, F.P.; resources, G.W. and Y.G.; data curation, F.P.; writing—original draft preparation, F.P.; writing—review and editing, G.W.; visualization, F.P.; supervision, G.W. and Y.G.; project administration, G.W. and Y.G.; funding acquisition, Y.G. All authors have read and agreed to the published version of the manuscript.

Funding: This work was supported by National Natural Science Foundation of China with Contract Nos. 12275307, 11575238, 11475222, 11505228, 10975159, 11275232, and 11735016, the National MCF Energy R&D Program (2019YFE03040000, 2019YFE03030000), the Research Project of Huainan Normal University (2020XJZD011).

Data Availability Statement: No data, models, or code were generated or used during the study.

Acknowledgments: Most numerical calculations in this paper have been done on the supercomputing system in the Supercomputing Center of University of Science and Technology of China, and the ShenMa High Performance Computing Cluster in Institute of Plasma Physics, Chinese Academy of Sciences.

Conflicts of Interest: The authors declare no conflict of interest.

References

1. Guo, H.D.; Xia, T.C.; Hu, B.B. High-order lumps, high-order breathers and hybrid solutions for an extended (3+1)-dimensional Jimbo-Miwa equation in fluid dynamics. *Nonlinear Dyn.* **2020**, *100*, 601–614. [CrossRef]
2. Lan, Z.Z.; Guo, B.L. Nonlinear waves behaviors for a coupled generalized nonlinear Schrodinger-Boussinesq system in a homogeneous magnetized plasma. *Nonlinear Dyn.* **2020**, *100*, 3771–3784. [CrossRef]
3. Biswas, A.; Ekici, M.; Sonmezoglu, A.; Belic, M.R. Solitons in optical fiber Bragg gratings with dispersive reflectivity by extended trial function method. *Optik* **2019**, *182*, 88–94. [CrossRef]
4. Seadawy, A.R.; Lu, D.C.; Nasreen, N.; Nasreen, S. Structure of optical solitons of resonant Schrodinger equation with quadratic cubic nonlinearity and modulation instability analysis. *Phys. A Stat. Mech. Its Appl.* **2019**, *534*, 122155. [CrossRef]
5. Abdoud, M.A.; Owyed, S.; Abdel-Aty, A.; Raffan, B.M.; Abdel-Khalek, S. Optical soliton solutions for a space-time fractional perturbed nonlinear Schrödinger equation arising in quantum physics. *Results Phys.* **2020**, *16*, 102895. [CrossRef]

6. Peng, W.Q.; Tian, S.F.; Zhang, T.T. Dynamics of the soliton waves, breather waves, and rogue waves to the cylindrical Kadomtsev-Petviashvili equation in pair-ion-electron plasma. *Phys. Fluids* **2019**, *31*, 102107. [CrossRef]
7. Liu, J.B.; Yang, K.Q. The extended F-expansion method and exact solutions of nonlinear PDEs. *Chaos Solitons Fractals* **2004**, *22*, 111. [CrossRef]
8. Zhang, S. Application of Exp-function method to a KdV equation with variable coefficients. *Phys. Lett. A* **2007**, *365*, 448. [CrossRef]
9. Zhang, S. The periodic wave solutions for the (2+1)-dimensional Konopelchenko–Dubrovsky equations. *Chaos Solitons Fractals* **2006**, *30*, 1213. [CrossRef]
10. Zhang, S. The periodic wave solutions for the (2+1)-dimensional dispersive long water equations. *Chaos Solitons Fractals* **2007**, *32*, 847. [CrossRef]
11. Abdou, M.A. The extended F-expansion method and its application for a class of nonlinear evolution equations. *Chaos Solitons Fractals* **2007**, *31*, 95. [CrossRef]
12. Wazwaz, A.M. The extended tanh method for new solitons solutions for many forms of the fifth-order KdV equations. *Appl. Math. Comput.* **2007**, *184*, 1002–1014. [CrossRef]
13. Wazwaz, A.M. The tanh–coth method for solitons and kink solutions for nonlinear parabolic equations. *Appl. Math. Comput.* **2007**, *188*, 1467–1475. [CrossRef]
14. Fan, E. Extended tanh-function method and its applications to nonlinear equations. *Phys. Lett. A* **2000**, *277*, 212. [CrossRef]
15. Liu, S.K.; Fu, Z.T.; Liu, S.D.; Zhao, Q. Jacobi elliptic function expansion method and periodic wave solutions of nonlinear wave equations. *Phys. Lett. A* **2001**, *289*, 69. [CrossRef]
16. Liu, S.K.; Fu, Z.T.; Liu, S.D.; Zhao, Q. New Jacobi elliptic function expansion and new periodic solutions of nonlinear wave equations. *Phys. Lett. A* **2001**, *290*, 72. [CrossRef]
17. Elgarayhi, A. New periodic wave solutions for the shallow water equations and the generalized Klein–Gordon equation. *Commun. Nonlinear Sci. Numer. Simul.* **2008**, *13*, 877–888. [CrossRef]
18. Wu, G.; Guo, Y. New Complex Wave Solutions and Diverse Wave Structures of the (2+1)-Dimensional Asymmetric Nizhnik–Novikov–Veselov Equation. *Fractal Fract.* **2023**, *7*, 170. [CrossRef]
19. Wu, G.; Han, J.; Zhang, W.; Zhang, M. New periodic wave solutions to nonlinear evolution equations by the extended mapping method. *Physical D-Nonlinear Phenom.* **2007**, *229*, 116. [CrossRef]
20. Sirendaoreji; Jiong, S. Auxiliary equation method for solving nonlinear partial differential equations. *Phys. Lett. A* **2003**, *309*, 387. [CrossRef]
21. Sirendaoreji. New exact travelling wave solutions for the Kawahara and modified Kawahara equations. *Chaos Solitons Fractals* **2004**, *19*, 147. [CrossRef]
22. Zhu, X.; Cheng, J.; Chen, Z.; Wu, G. New Solitary-Wave Solutions of the Van der Waals Normal Form for Granular Materials via New Auxiliary Equation Method. *Mathematics* **2022**, *10*, 2560. [CrossRef]
23. Wu, G.; Guo, Y. Construction of New Infinite-Series Exact Solitary Wave Solutions and Its Application to the Korteweg–De Vries Equation. *Fractal Fract.* **2023**, *7*, 75. [CrossRef]
24. Wang, M.L. Solitary wave solutions for variant Boussinesq equations. *Phys. Lett. A* **1995**, *199*, 169–172. [CrossRef]
25. Wang, M.L.; Zhou, Y.B.; Li, Z.B. Application of a homogenous balance method to exact solitons of nonlinear equations in mathematical physics. *Phys. Lett. A* **1996**, *216*, 67–75. [CrossRef]
26. Otwinowski, M.; Paul, R. Laidlaw WG. Exact travelling wave solutions of a class of nonlinear diffusion equations by reduction to a quadrature. *Phys. Lett. A* **1988**, *128*, 483–487. [CrossRef]
27. Wang, M.; Li, X.; Zhang, J. The (G′/G)-expansion method and travelling wave solutions of nonlinear evolution equations in mathematical physics. *Phys. Lett. A* **2008**, *372*, 417. [CrossRef]
28. Zayed, E.M.E.; Gepreel, K.A. The G′/G-expansion method for finding the traveling wave solutions of nonlinear partial differential equations in mathematical physics. *J. Math. Phys.* **2009**, *50*, 013502. [CrossRef]
29. Guo, S.; Zhou, Y. The extended G′/G -expansion method and its applications to the Whitham–Broer–Kaup–Like equations and coupled Hirota–Satsuma KdV equations. *Appl. Math. Comput.* **2010**, *215*, 3214. [CrossRef]
30. Islam, M.S.; Khan, K.; Akbar, M.A. An analytical method for finding exact solutions of modified Korteweg–de Vries equation. *Results Phys.* **2015**, *5*, 131. [CrossRef]
31. Kadomtsev, B.B.; Petviashvili, V.I. On the stability of solitary waves in weakly dispersing media. *Sov. Phys. Dokl.* **1970**, *15*, 539–554.
32. Segur, H.; Finkel, A. An analytical model of periodic waves in shallow water. *Stud. Appl. Math.* **1985**, *73*, 183–220. [CrossRef]
33. Hammack, J.; Scheffner, N.; Segur, H. Two-dimensional periodic waves in shallow water. *J. Fluid Mech.* **1989**, *209*, 567–589. [CrossRef]
34. Hammack, J.; Scheffner, N.; Segur, H. Two-dimensional periodic waves in shallow water. Part 2. Asymmetric waves. *J. Fluid Mech.* **1995**, *285*, 95–122. [CrossRef]
35. Infeld, E.; Rowlands, G. *Nonlinear Waves, Solitons and Chaos*; Cambridge University Press: Cambridge, UK, 2000.
36. Pelinovsky, D.E.; Stepanyants, Y.A.; Kivshar, Y.S. Self-focusing of plane dark solitons in nonlinear defocusing media. *Phys. Rev. E* **1995**, *51*, 5016–5026. [CrossRef] [PubMed]
37. Baronio, F.; Wabnitz, S.; Kodama, Y. Optical Kerr spatio-temporal dark-lump dynamics of hydrodynamic origin. *Phys. Rev. Lett.* **2016**, *116*, 173901. [CrossRef]

38. Tajiri, M.; Murakami, Y. Two-Dimensional Multisoliton Solutions: Periodic Soliton Solutions to the Kadomtsev-Petviashvili Equation with Positive Dispersion. *J. Phys. Soc. Jpn.* **1989**, *58*, 3029–3032. [CrossRef]
39. Manakov, S.; Zakharov, V.; Bordag, L.; Its, A.; Matveev, V. Two-dimensional solitons of the Kadomtsev-Petviashvili equation and their interaction. *Phys. Lett. A* **1977**, *63*, 205–206. [CrossRef]
40. Johnson, R.; Thompson, S. A solution of the inverse scattering problem for the Kadomtsev-Petviashvili equation by the method of separation of variables. *Phys. Lett. A* **1978**, *66*, 279–281. [CrossRef]
41. Tajiri, M.; Fujimura, Y.; Murakami, Y. Resonant Interactions between Y-Periodic Soliton and Algebraic Soliton: Solutions to the Kadomtsev-Petviashvili Equation with Positive Dispersion. *J. Phys. Soc. Jpn.* **1992**, *61*, 783–790. [CrossRef]
42. Murakami, Y.; Tajiri, M. Resonant Interaction between Line Soliton and Y-Periodic Soliton: Solutions to the Kadomtsev-Petviashvili Equation with Positive Dispersion. *J. Phys. Soc. Jpn.* **1992**, *61*, 791–805. [CrossRef]
43. Klein, C.; Saut, J.-C. Numerical Study of Blow up and Stability of Solutions of Generalized Kadomtsev–Petviashvili Equations. *J. Nonlinear Sci.* **2012**, *22*, 763–811. [CrossRef]
44. Chakravarty, S.; Zowada, M. Multi-lump wave patterns of KPI via integer partitions. *Phys. D Nonlinear Phenom.* **2023**, *446*, 133644. [CrossRef]
45. Kim, V.A.; Parovik, R.I.; Rakhmonov, Z.R. Implicit Finite-Difference Scheme for a Duffing Oscillator with a Derivative of Variable Fractional Order of the Riemann-Liouville Type. *Mathematics* **2023**, *11*, 558. [CrossRef]
46. Loi, W.S.; Ong, C.T. Optical solitons: Mathematical model and simulations. In Proceedings of the 2013 IEEE Business Engineering and Industrial Applications Colloquium (BEIAC), Langkawi, Malaysia, 7–9 April 2013; 2013; pp. 901–905. [CrossRef]
47. Fedoruk, M.P. Mathematical modeling of optical communication lines with dispersion management. In *Computational Science and High Performance Computing. Notes on Numerical Fluid Mechanics and Multidisciplinary Design (NNFM)*; Krause, E., Shokin, Y.I., Resch, M., Shokina, N., Eds.; Springer: Berlin/Heidelberg, Germany, 2005; Volume 88. [CrossRef]